



# $\Lambda$ hyperon yields in carbon-nucleus interactions

A.Zinchenko, M.Kapishin,  
G.Pokatashkin, I.Rufanov, V.Vasendina

*for the BM@N collaboration  
VBLHEP, JINR, Dubna, Russia*



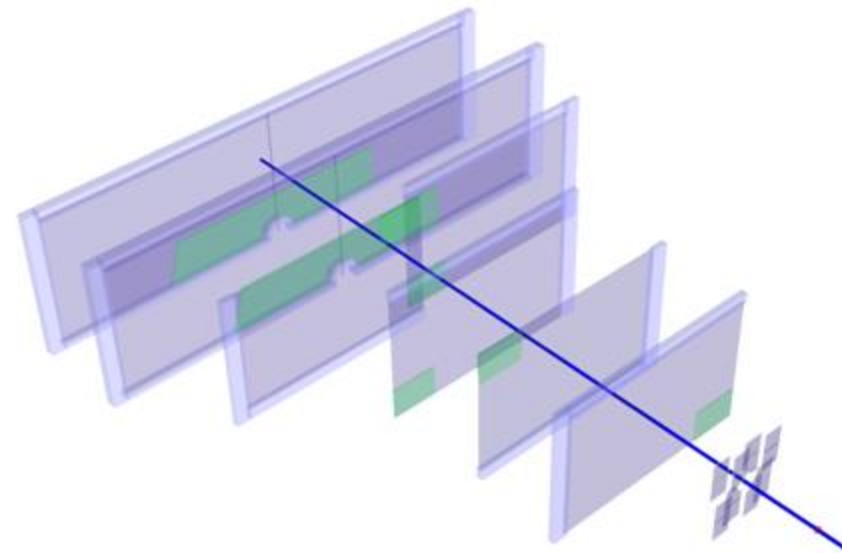
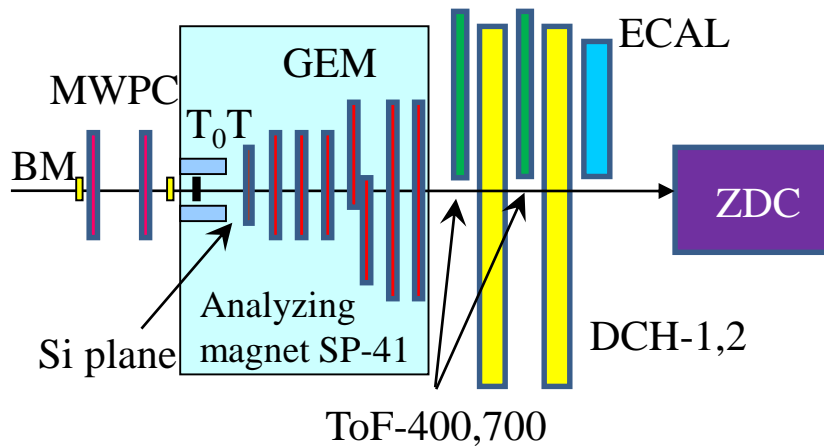
**Joint Institute for Nuclear  
Research**

SCIENCE BRINGING NATIONS  
TOGETHER

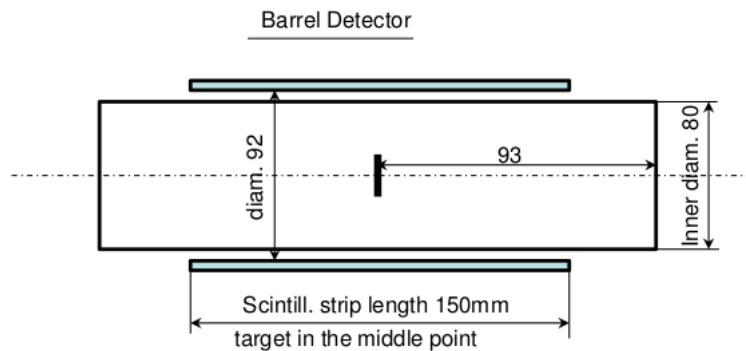
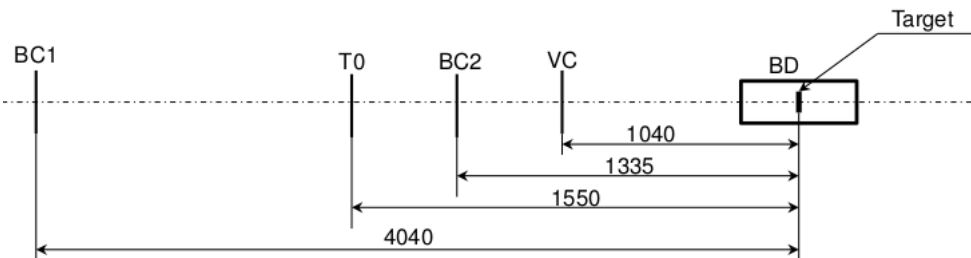
4th BM@N collaboration meeting  
15.10.2019

1. Run with carbon beam (March 2017)
  - ✓ BM@N detector set-up
2. Data analysis ( $C+C$ ,  $C+Al$ ,  $C+Cu$ ,  $C+Pb$  at 4A GeV and 4.5A GeV)
  - ✓ Selection criteria
  - ✓ Reconstructed signal of  $\Lambda$  ( $dN/dy$  &  $dN/p_T$  spectra)
  - ✓ Data - MC agreement: multiplicity, momentum spectra
  - ✓ Decomposition of  $\Lambda$  reconstruction efficiency
  - ✓ Cross section and yields of  $\Lambda$
  - ✓ Reconstructed  $p_T$  spectra of  $\Lambda$  and extracted temperature
  - ✓ Systematic errors
3. Summary

# BM@N set-up in carbon run



Central tracker in carbon run.



Schematic view and positions of the beam counters, barrel detector and target.

# Event selection criteria



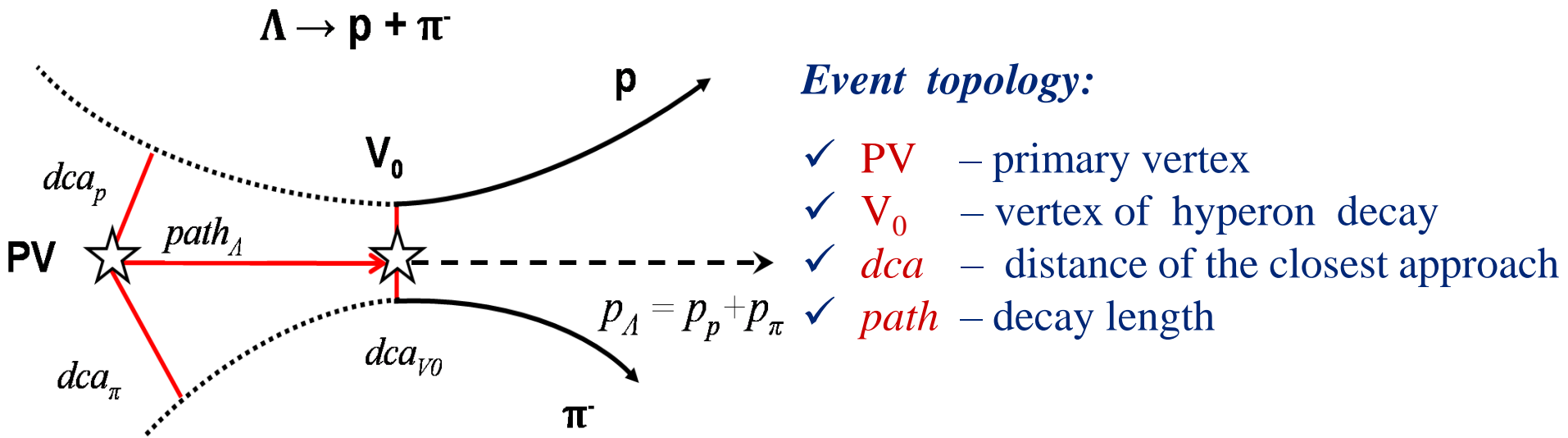
- ✓ Number of tracks in selected events: pos $\geq$ 1, neg $\geq$ 1;
- ✓ Beam halo, pile-up suppression within the readout time window: number of signals in the start detector: T0=1, number of signals in the beam counter: BC2=1, number of signals in the veto counter around the beam: Veto=0;
- ✓ Trigger condition in the barrel multiplicity detector: number of signals BD $\geq$ 2 or BD $\geq$ 3 (run dependent).

Selection	4AGeV	4.5AGeV
<b>T0==1</b>	+	+
<b>BC2==1</b>	+	+
<b>VETO==0</b>	+	+
<i>C</i>	<b>0.64</b>	<b>0.53</b>
<i>Al</i>	<b>0.74</b>	<b>0.58</b>
<i>Cu</i>	<b>0.78</b>	<b>0.62</b>
<i>Pb</i>	-	<b>0.68</b>

**Table.** Number of triggered events, beam fluxes and integrated luminosities collected in the carbon beam of 4.5A GeV (4A GeV).

Interactions (target thickness)	Number of triggers / $10^6$	Integrated beam flux / $10^7$	Integrated luminosity / $10^{30} \text{ cm}^{-2}$
<i>C+C</i> (9mm)	2.75(4.57)	4.53(6.99)	4.52(7.16)
<i>C+Al</i> (12mm)	3.23(5.35)	4.53(4.41)	3.27(3.11)
<i>C+Cu</i> (5mm)	3.76(5.31)	5.22(4.57)	2.22(1.98)
<i>C+Pb</i> (9.9mm)	2.36	2.62	0.86

# $\Lambda$ hyperon selection criteria



- ✓ Number of hits in 1 Si + 6 GEM per track > 3
- ✓ Momentum range of positive tracks:  $0.5 < p_{pos} < 4.5$  GeV/c
- ✓ Momentum range of negative tracks:  $0.1 < p_{neg} < 2.5$  GeV/c
- ✓ Distance of minimum approach of *V0* tracks:  $dca < 1$  cm
- ✓ Distance between *V0* and primary vertex:  $path > 2.5$  cm

# Signal of $\Lambda$ in $C+C$ , $C+Al$ , $C+Cu$ , $C+Pb$ interactions

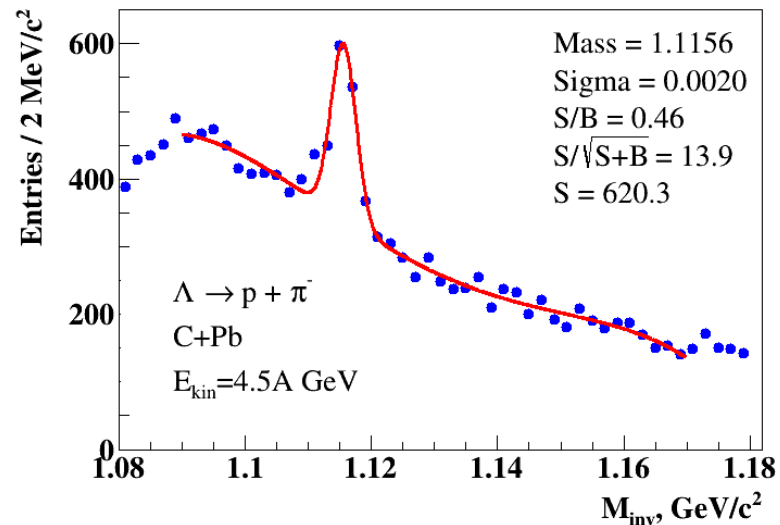
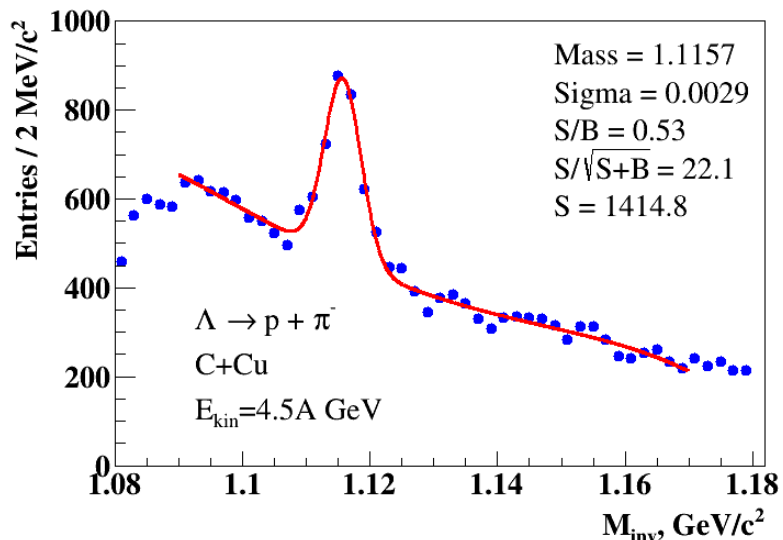
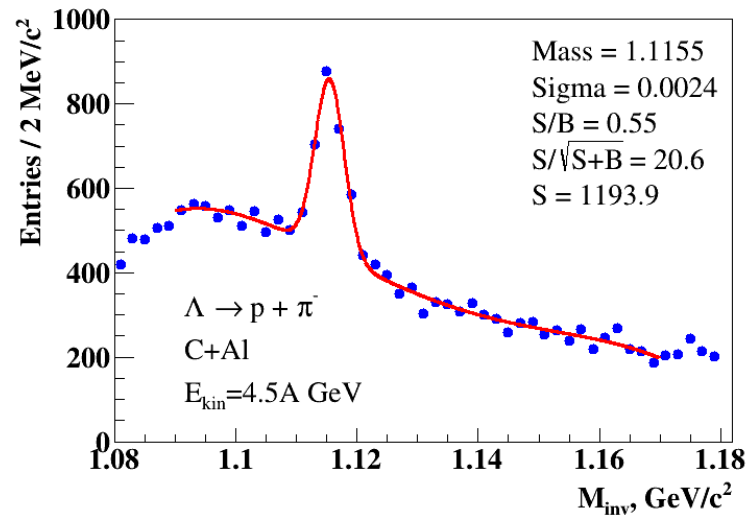
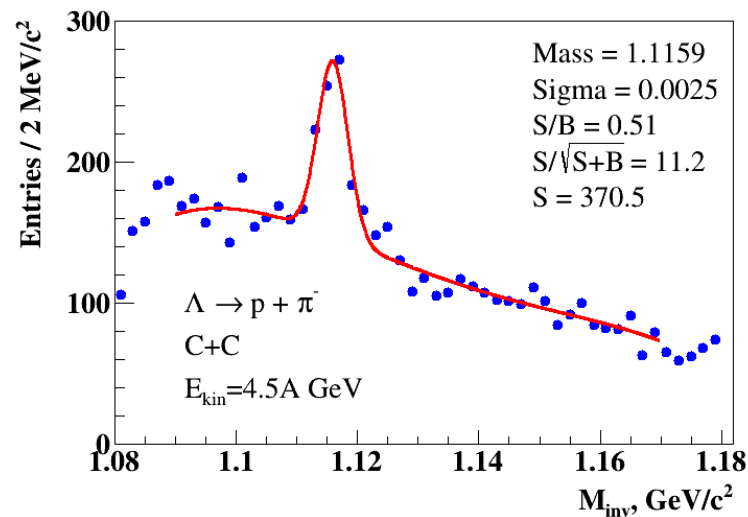


**Fig.**  $\Lambda \rightarrow p\pi$  signal reconstructed in interactions of the carbon beam with targets:  $C$ ,  $Al$ ,  $Cu$ ,  $Pb$ .

# Comparison of experimental data and MC

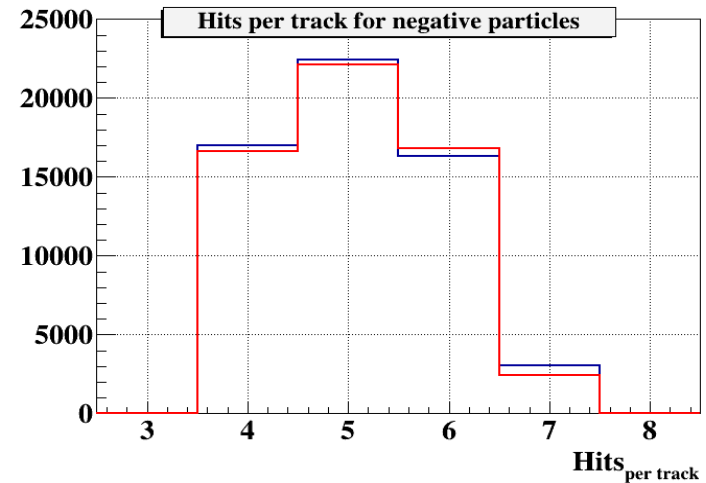
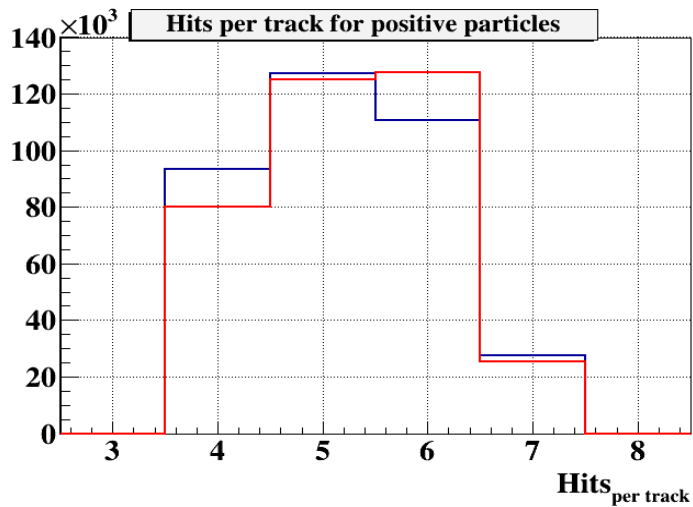
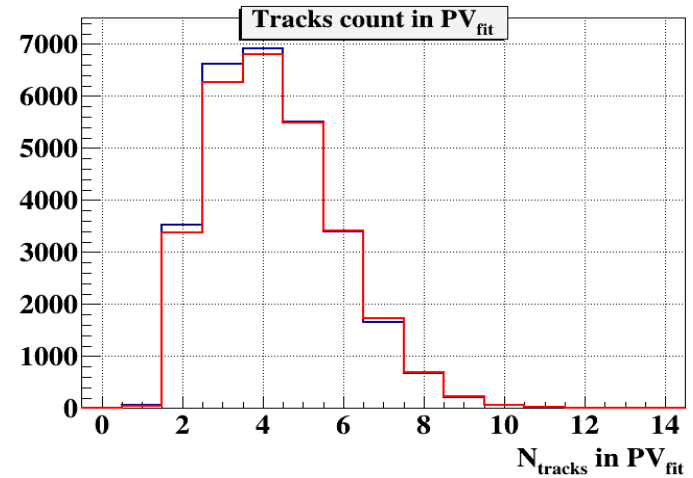
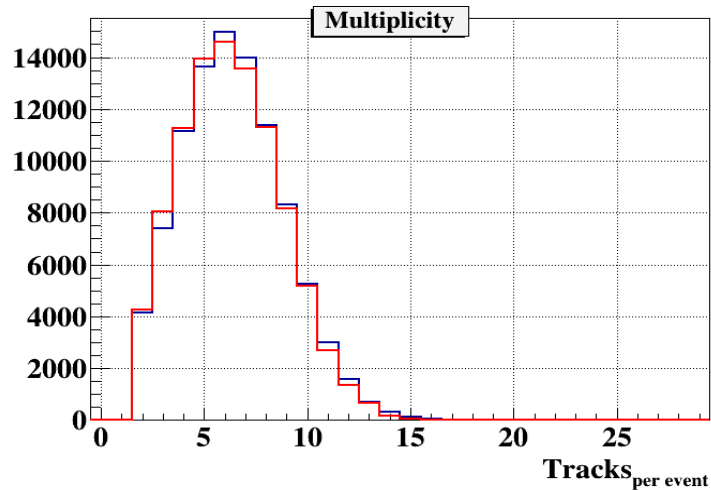


**Fig.** Comparison of experimental distributions (red lines) and MC (DCM-QGSM) (blue curves) in  $C+Cu$  interaction: track multiplicity per event; number of tracks reconstructed in the primary vertex; number of hits per positive particle reconstructed in 1 Si + 6 GEM detectors; number of hits per negative particle.

# Comparison of experimental data and MC

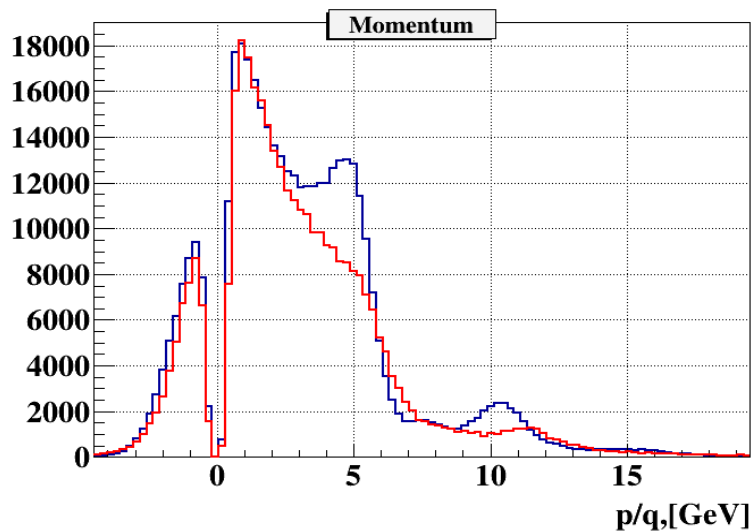
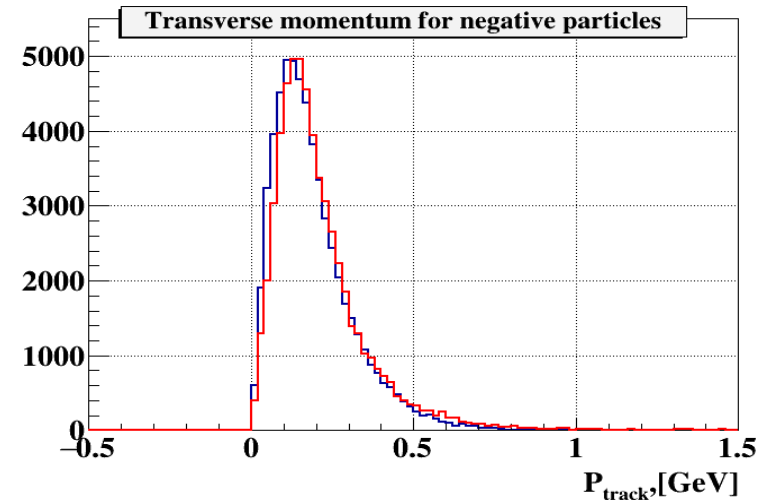
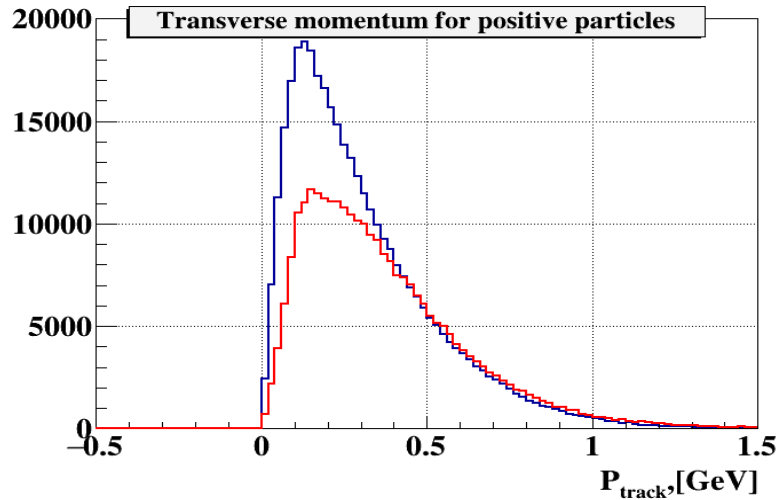


**Fig.** Comparison of experimental data (red curves) and MC (DCM-QGSM) simulation (blue curves) in  $C+Cu$  interaction: transverse momentum of positive particles; transverse momentum of negative particles; total momentum of negative ( $p/q < 0$ ) and positive particles ( $p/q > 0$ ).



**Table.** Decomposition of  $\Lambda$  reconstruction efficiency.

Reconstruction efficiency	$\varepsilon_{rec} = \varepsilon_{acc} \cdot \varepsilon_{emb} \cdot \varepsilon_{cuts}$
$\Lambda$ geometrical acceptance in GEM detectors	$\varepsilon_{acc} = N_{acc}(y, p_T) / N_{gen}(y, p_T)$
Efficiency of reconstruction of embedded $\Lambda$	$\varepsilon_{emb} = N_{emb}(y, p_T) / N_{acc}(y, p_T)$
Efficiency of $\Lambda$ selection: kinematical and spatial cuts	$\varepsilon_{cuts} = N_{rec}(y, p_T) / N_{emb}(y, p_T)$

# Efficiency in $C+Cu$ interaction

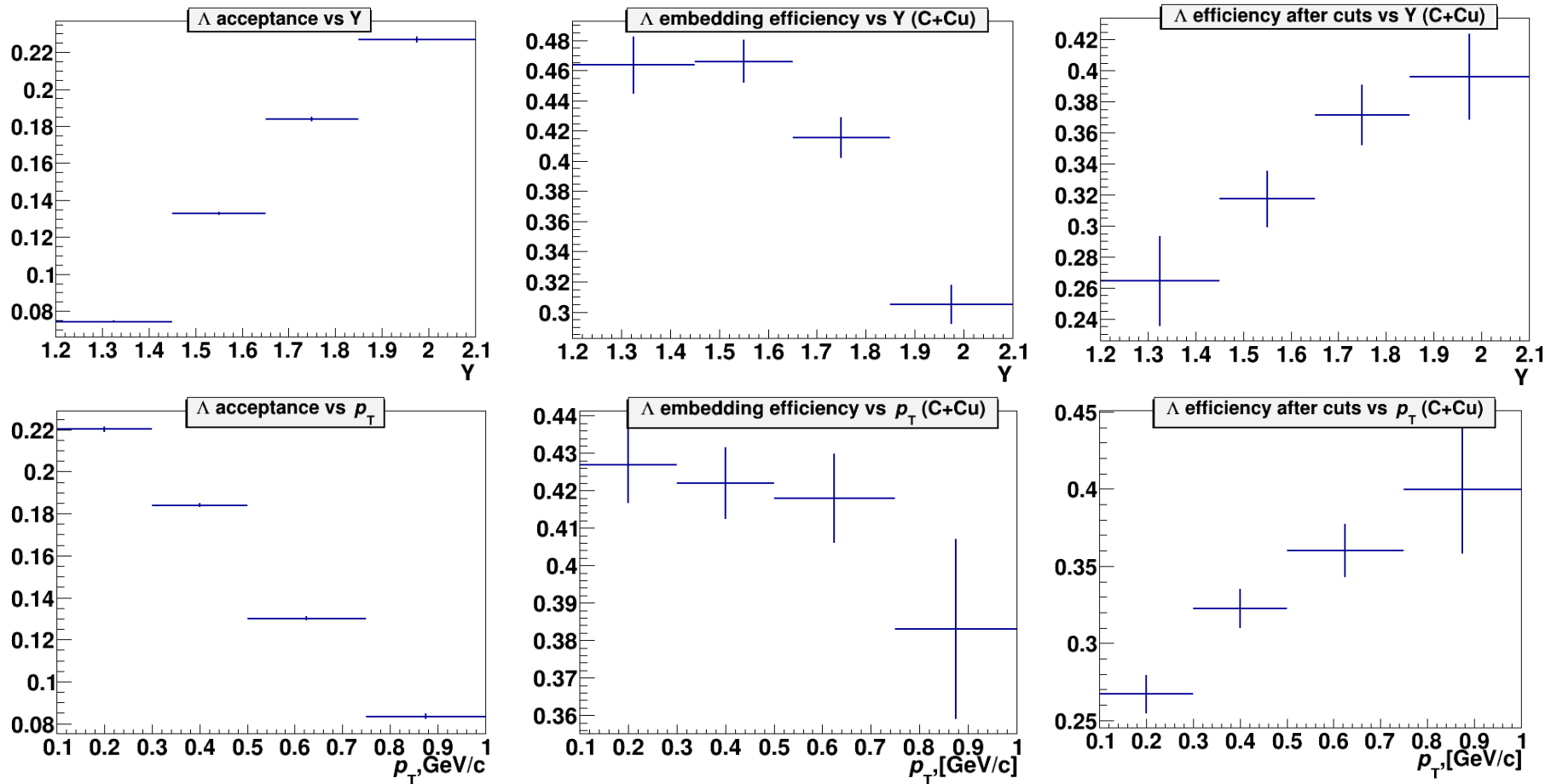


**Fig.**  $\Lambda$  geometrical acceptance ( $\epsilon_{acc}$ ); efficiency of reconstruction of embedded  $\Lambda$  ( $\epsilon_{emb}$ ); efficiency of kinematical and spatial cuts applied for  $\Lambda$  reconstruction ( $\epsilon_{cuts}$ ) as functions of rapidity  $y$  (top plots) and  $p_T$  (bottom plots). Results are shown for  $C+Cu$  interaction.

# Efficiency in $C+Cu$ interaction

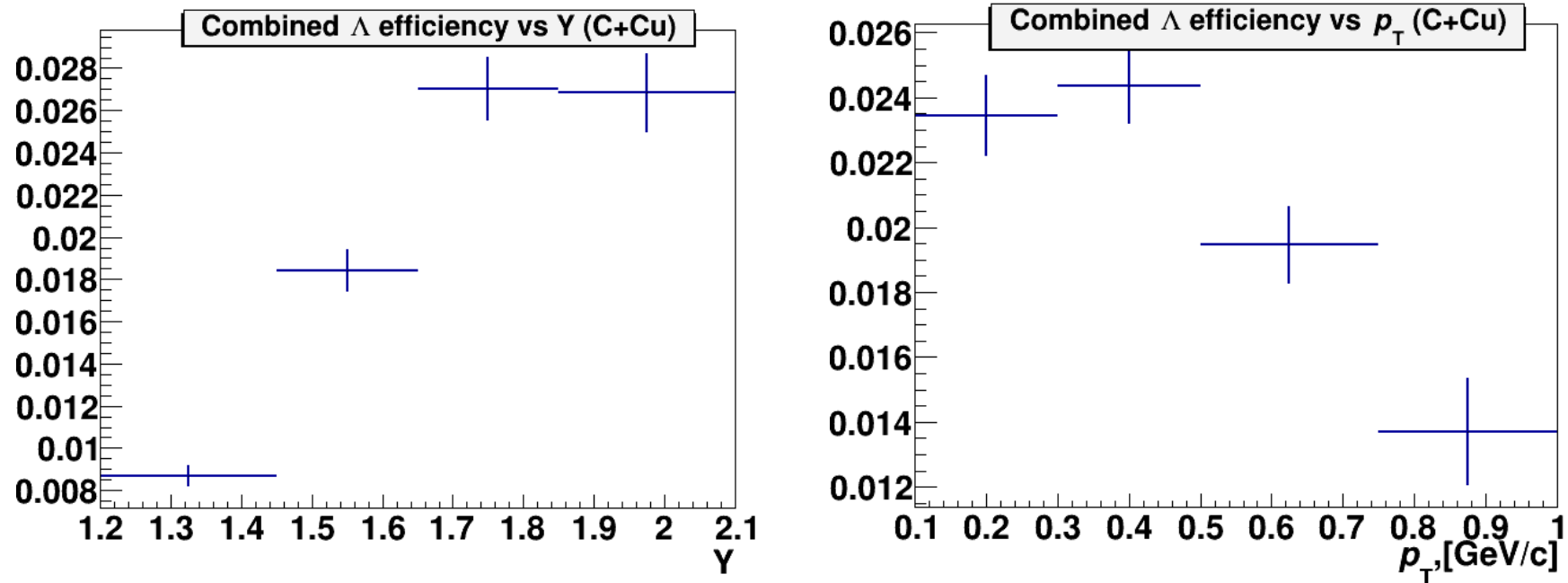


**Fig.** Combined  $\Lambda$  efficiency as functions of rapidity  $y$  (left plot) and  $p_T$  (right plot).

# Cross section and yields of $\Lambda$ hyperon



The cross section  $\sigma_{\Lambda}$  and yield  $Y_{\Lambda}$  of  $\Lambda$  hyperon production in  $C+C$ ,  $C+Al$ ,  $C+Cu$ ,  $C+Pb$  interactions are calculated in bins of  $y$  and  $p_T$  according to the formulae:

$$\sigma_{\Lambda}(y,p_T) = N_{rec}^{\Lambda}(y,p_T) / (\varepsilon_{rec}(y,p_T) \cdot \varepsilon_{trig} \cdot L); \quad Y_{\Lambda}(y,p_T) = \sigma_{\Lambda}(y,p_T) / \sigma_{inel}$$

where  $L$  is the luminosity,

$N_{rec}^{\Lambda}$ —the number of reconstructed  $\Lambda$  hyperons,

$\varepsilon_{rec}$ —the combined efficiency of the  $\Lambda$  hyperon reconstruction,

$\varepsilon_{trig}$ —the trigger efficiency,

$\sigma_{inel}$ — the cross section for minimum bias inelastic  $C+A$  interactions.

Interaction	$C+C$	$C+Al$	$C+Cu$	$C+Pb$
Inelastic cross section, mb	830±50	1260±50	1790±50	3075±50

The cross sections for inelastic  $C+Al$ ,  $C+Cu$ ,  $C+Pb$  interactions are taken from the predictions of the DCM-QGSM model which are consistent with the results calculated by the formula:  $\sigma_{inel} = \pi R_0^2 (A_P^{1/3} + A_T^{1/3})^2$ , where  $R_0 = 1.2$  fm is an effective nucleon radius,  $A_P$  and  $A_T$  are atomic numbers of the beam and target nucleus.

# Yields of $\Lambda$ hyperons in 4A GeV C+A (updated)

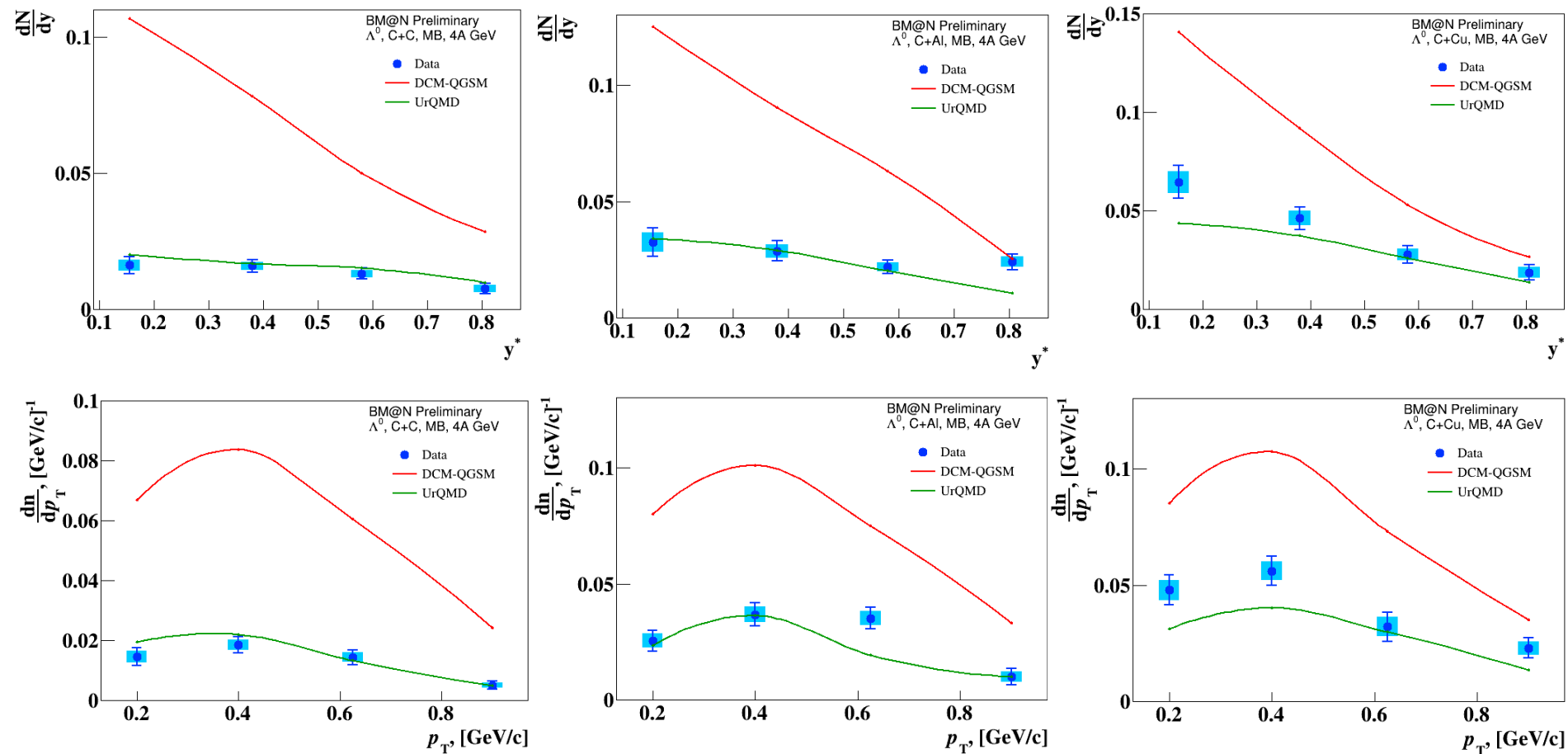


**Fig.** Reconstructed yields of  $\Lambda$  hyperons in minimum bias C+C, C+Al, C+Cu interactions vs rapidity  $y$  and transverse momentum  $p_T$  for 4A GeV.

# Yields of $\Lambda$ hyperons in 4.5A GeV C+A

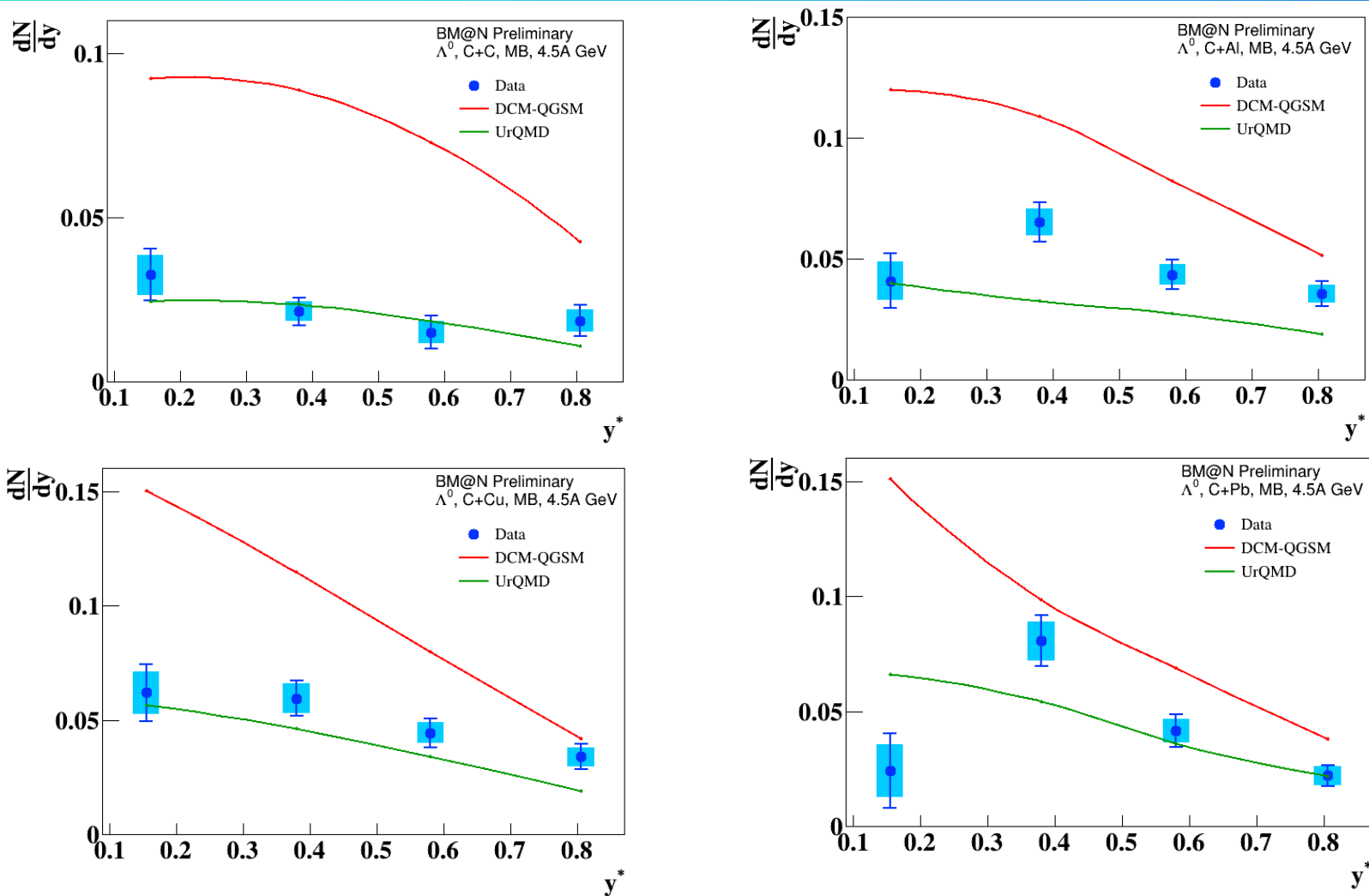


**Fig.** Reconstructed yields of  $\Lambda$  hyperons in minimum bias C+C, C+Al, C+Cu, C+Pb interactions vs rapidity  $y$  for 4.5A GeV.

# Yields of $\Lambda$ hyperons in 4.5A GeV C+A

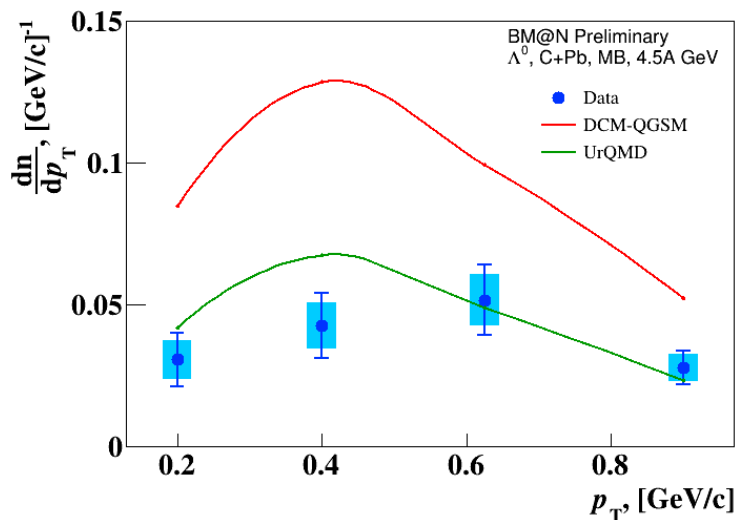
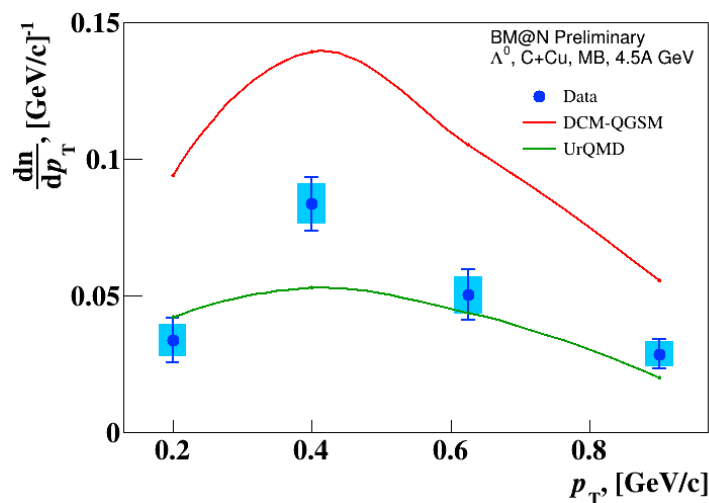
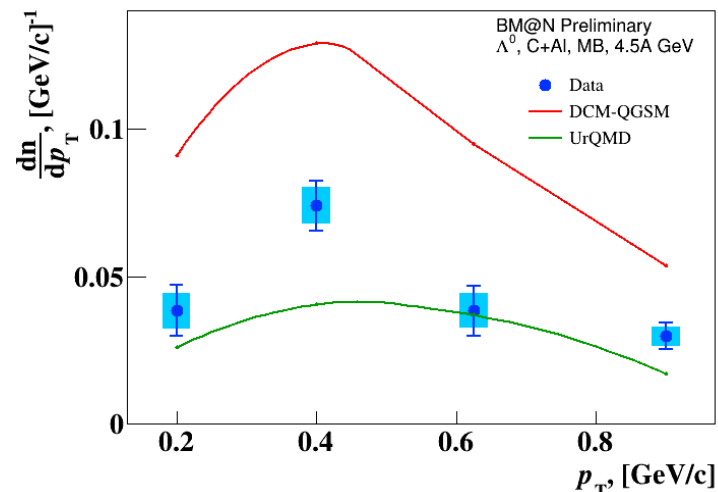
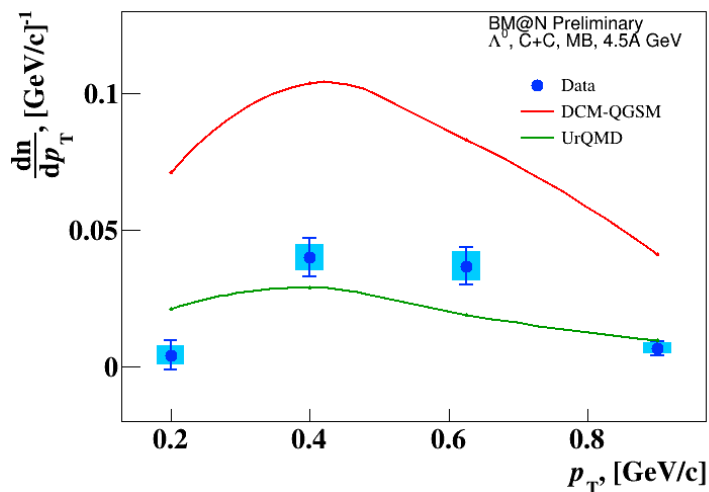
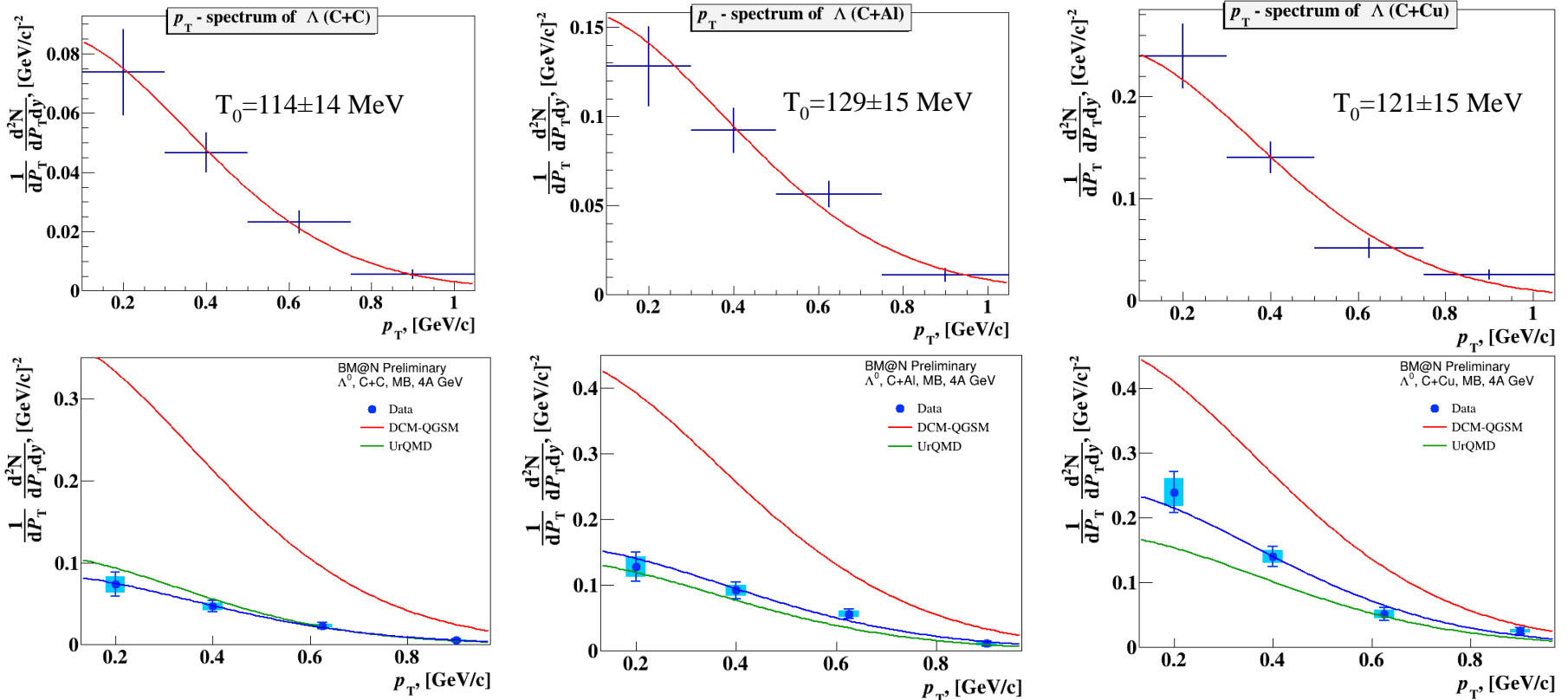


**Fig.** Reconstructed yields of  $\Lambda$  hyperons in minimum bias C+C, C+Al, C+Cu, C+Pb interactions vs transverse momentum  $p_T$  for 4.5A GeV.

# $p_T$ spectra of $\Lambda$ and $T_0$ slope in 4A GeV C+A (updated)

**Table.** Temperature parameter extracted from the fit of the  $p_T$  spectra.

	$T_0$ , MeV (C+C)	$T_0$ , MeV (C+Al)	$T_0$ , MeV (C+Cu)
Experiment	$114 \pm 14 \pm 9$	$129 \pm 15 \pm 10$	$121 \pm 15 \pm 10$
DCM-QGSM	115	122	121
UrQMD	100	118	124



**Fit of invariant  $p_T$  spectra of  $\Lambda$  yields in C+C, C+Al, C+Cu minimum bias interactions by function:**  
 $1/p_T \cdot d^2N/dp_T dy = A \cdot \exp(-(mT - m\Lambda)/T)$ ,  $mT = \sqrt{(m\Lambda^2 + pT^2)}$



# $p_T$ spectra of $\Lambda$ and $T_0$ slope in 4.5 AGeV C+A

**Table.** Temperature parameter extracted from the fit of the  $p_T$  spectra.

	$T_0$ , MeV (C+C)	$T_0$ , MeV (C+Al)
Experiment	$137 \pm 20 \pm 15$	$147 \pm 18 \pm 9$
DCM-QGSM	140	142
UrQMD	125	150

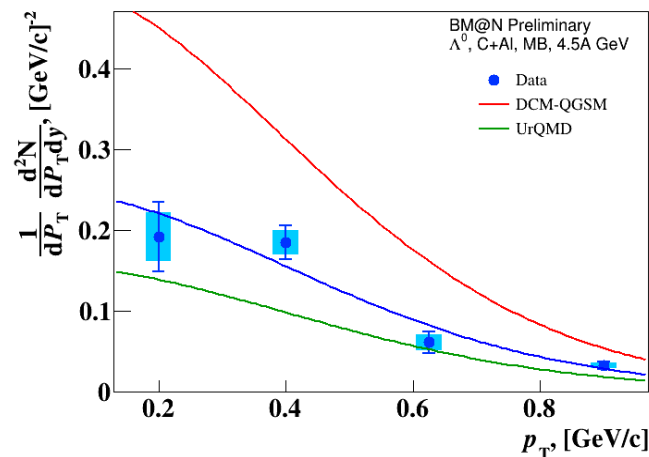
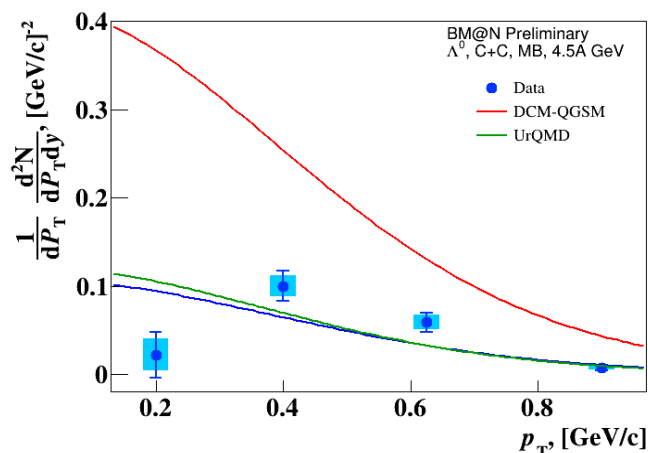
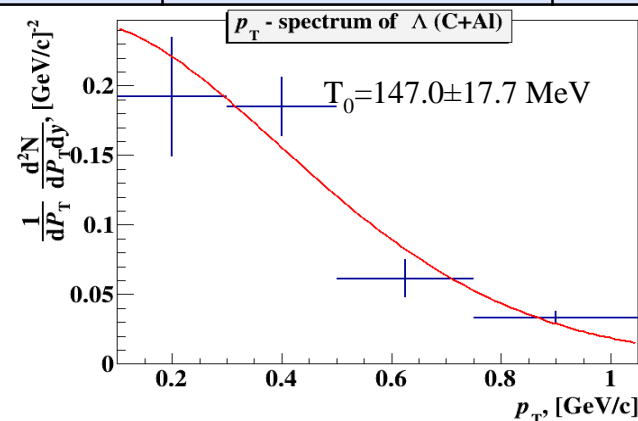
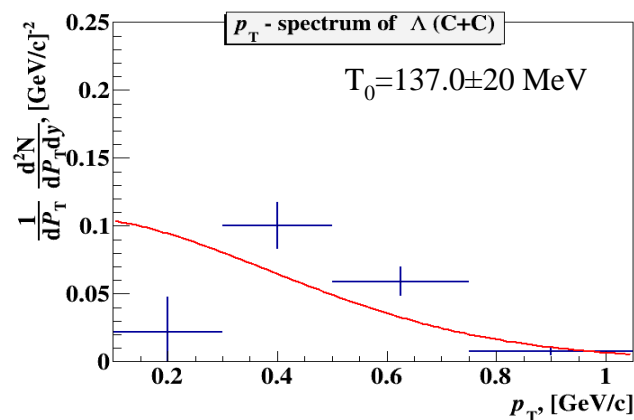


**Fig.** Thermal fit results with the inverse slope parameter  $T_0$ : data and predictions of models for 4.5A GeV.

# $p_T$ spectra of $\Lambda$ and $T_0$ slope in 4.5 AGeV C+A

**Table.** Temperature parameter extracted from the fit of the  $p_T$  spectra.

	$T_0$ , MeV (C+Cu)	$T_0$ , MeV (C+Pb)
Experiment	$149 \pm 18 \pm 12$	$188 \pm 38 \pm 26$
DCM-QGSM	141	145
UrQMD	131	136

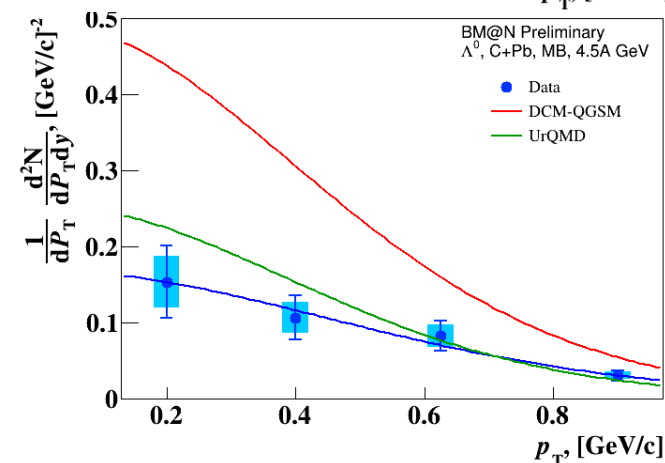
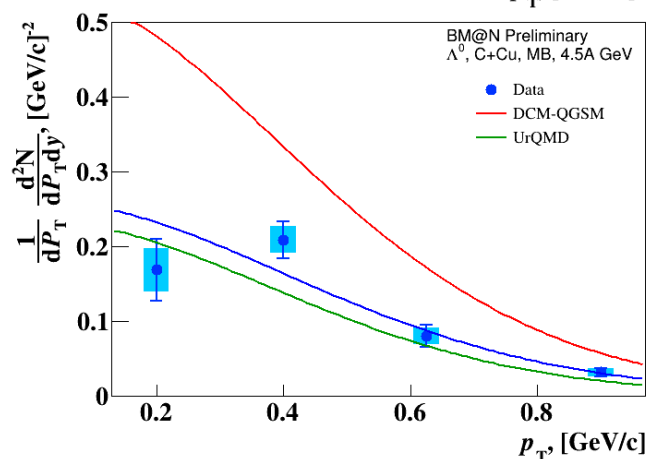
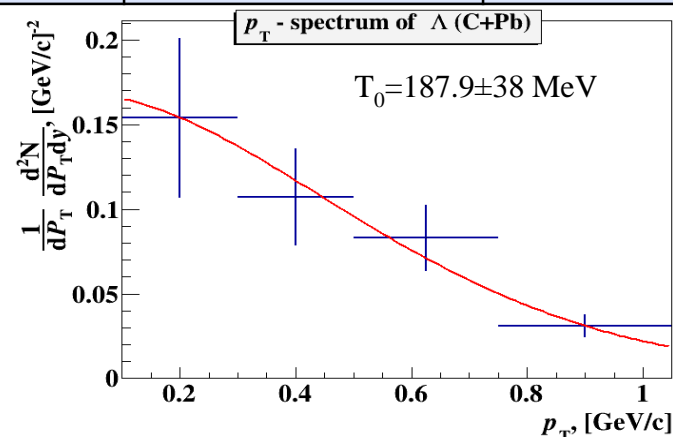
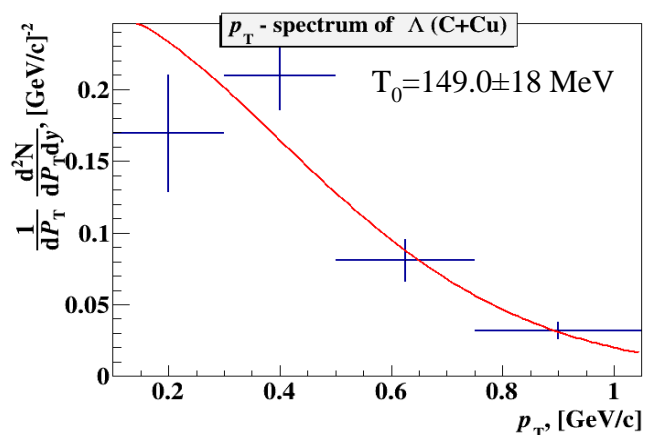


**Fig.** Thermal fit results with the inverse slope parameter  $T_0$ : data and predictions of models for 4.5A GeV.

# Systematic errors



**Table.** Total systematic uncertainty of the yield for 4A GeV.

Target Interval	y			Target Interval	p <sub>T</sub>		
	C, sys%	Al, sys%	Cu, sys%		C, sys%	Al, sys%	Cu, sys%
1.2-1.45	13.5	13.3	10.0	0.1-0.3	17.4	12.6	8.6
1.45-1.65	11.1	11.0	9.4	0.3-0.55	11.6	11.1	8.5
1.65-1.85	13.5	11.0	14.2	0.55-0.8	12.4	9.6	17.0
1.85-2.1	23.7	12.5	13.5	0.8-1.05	21.3	26.8	15.4

**Table.** Total systematic uncertainty of the yield for 4.5A GeV.

Target Interval	y				Target Interval	p <sub>T</sub>			
	C, sys%	Al, sys%	Cu, sys%	Pb, sys%		C, sys%	Al, sys%	Cu, sys%	Pb, sys%
1.2-1.45	18.7	19.2	17.8	47.8	0.1-0.3	55.0	15.7	16.5	22.2
1.45-1.65	13.6	8.7	9.9	10.4	0.3-0.55	12.1	7.6	8.5	19.6
1.65-1.85	22.8	10.1	10.5	12.6	0.55-0.8	14.5	11.0	14.4	17.9
1.85-2.1	18.3	10.3	11.3	18.8	0.8-1.05	29.9	12.9	14.8	16.2

Measured kinematic range:

\* Uncertainty of background under Lambda signal:  $\sqrt{(0.5 \cdot \text{bkg})}$

+ Uncertainty of background fit by Legendre(4) - Legendre(3)

\* Uncertainty of reconstruction efficiency (embedding+cuts) evaluated for different data runs

\* Uncertainty of trigger efficiency (2%)

Full kinematic range:

\* Extrapolation uncertainty to full kin. range (UrQMD;DCM-QGSM)

\* Uncertainty of C+A inelastic cross section

**Table.** Extrapolation factors to the full kinematic range, yields and cross sections.

	<i>C</i>	<i>Al</i>	<i>Cu</i>
DCM-QGSM URQMD extrapolation factors	6574/2474 1827/639	10539/3413 3248/1056	15817/3545 5509/1360
Yields in the measured kin range $0.1 < p_T < 1.05$ GeV/c, $1.2 < y_{lab} < 2.1$	$0.0118 \pm 0.0011 \pm 0.0009$	$0.0243 \pm 0.0020 \pm 0.0016$	$0.0362 \pm 0.0027 \pm 0.0021$
Yields in the full kinematic range N part DCM-QGSM	$0.0327 \pm 0.0030 \pm 0.0024$ 9	$0.0750 \pm 0.062 \pm 0.042$ 13.4	$0.154 \pm 0.011 \pm 0.009$ 23
<i>A</i> cross section in min. bias interactions, mb	$27.1 \pm 2.5$ (stat) $\pm 2.0$ (sys)	$94.5 \pm 8.0$ (stat) $\pm 6.1$ (sys)	$276 \pm 20$ (stat) $\pm 16$ (sys)

**Table.** Extrapolation factors to the full kinematic range, yields and cross sections.

	<i>C</i>	<i>Al</i>	<i>Cu</i>	<i>Pb</i>
DCM-QGSM URQMD extrapolation factors	3866/1581 1104/433	5447/1968 1955/671	8208/2222 3381/876	12324/2107 6404/1016
Yields in the measured kin range $0.1 < p_T < 1.05$ GeV/c, $1.2 < y_{lab} < 2.1$	$0.0202 \pm 0.0026$ $\pm 0.0020$	$0.0410 \pm 0.0037$ $\pm 0.0026$	$0.0446 \pm 0.0034$ $\pm 0.0031$	$0.0356 \pm 0.0047$ $\pm 0.0036$
Yields in the full kinematic range N part DCM-QGSM	$0.0504 \pm 0.0063$ $\pm 0.0049$	$0.116 \pm 0.010$ $\pm 0.007$	$0.169 \pm 0.013$ $\pm 0.012$	$0.216 \pm 0.028$ $\pm 0.022$
<i>A</i> cross section in min. bias interactions, mb	$41.8 \pm 5.3 \pm 4.0$	$147 \pm 13.0 \pm 9.0$	$302 \pm 23 \pm 20$	$665 \pm 87 \pm 64$

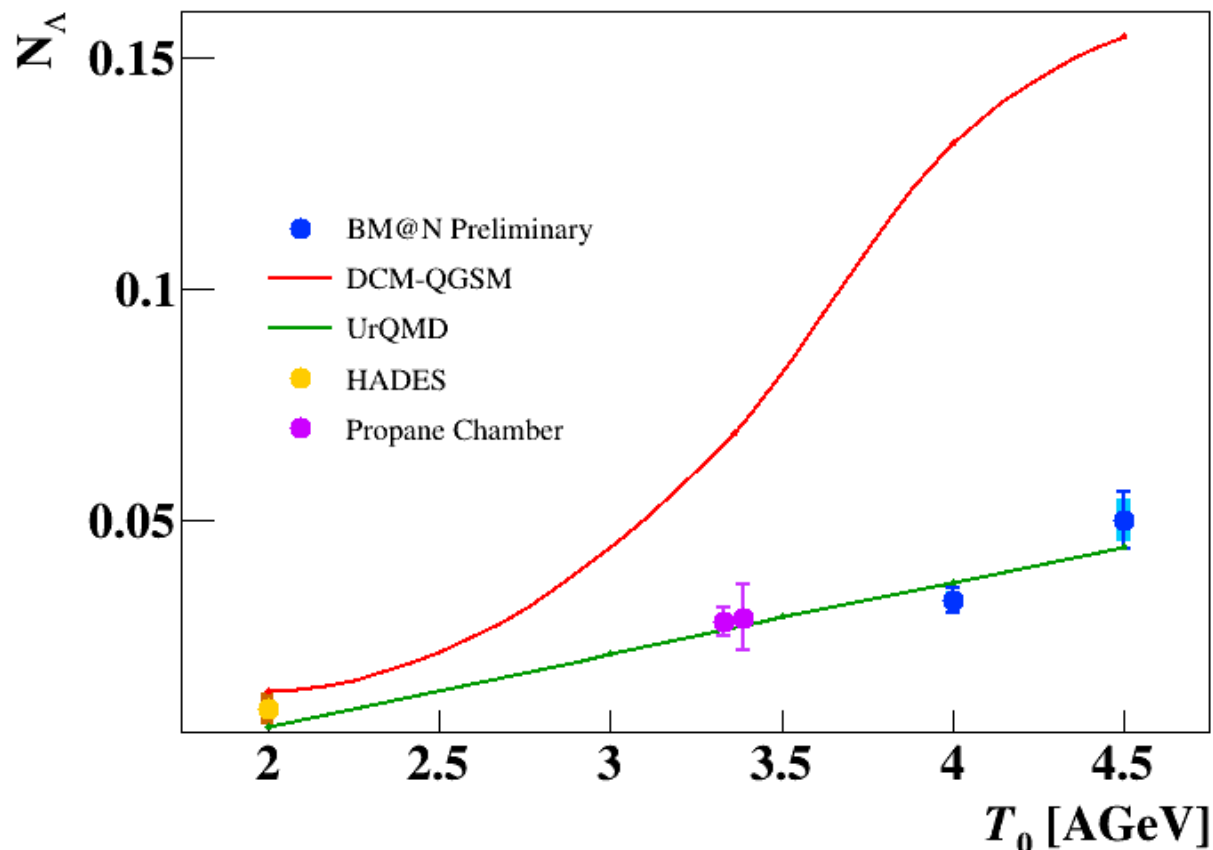


**Fig.** Energy dependence of  $\Lambda$  yields measured in different experiments. BM@N result is compared with data [S.Arakelian et al., P1-83-354, JINR, Dubna; D.Armutlijsky et al., P1-85-220, JINR, Dubna; Kalliopi Kanaki, PhD “Study of  $\Lambda$  hyperon production”]. The predictions of the DCM-QGSM and UrQMD models are shown.

1. Production of  $\Lambda$  hyperons in interactions of the 4A GeV and 4.5A GeV kinetic energy carbon beam with *C*, *Al*, *Cu*, *Pb* targets was studied with the BM@N detector at the Nuclotron.
2. The analysis procedure has been presented and described.
3. Results on  $\Lambda$  hyperon yields have been obtained and compared with model predictions and data available.
4. Analysis Note to be realized in a week.

Thank you for attention!

# Backup





**Table.** Comparison between  $A$  yields and cross sections for 4A GeV.

	$C$	$Al$	$Cu$
Yields in the measured kin range (current)	$0.0129 \pm 0.0011 \pm 0.0007$	$0.0243 \pm 0.0020 \pm 0.0014$	$0.0362 \pm 0.0027 \pm 0.0018$
Yields in the full kinematic range (current)	$0.0327 \pm 0.0028 \pm 0.0018$	$0.0759 \pm 0.062 \pm 0.044$	$0.154 \pm 0.011 \pm 0.008$
$A$ cross section, MB, mb (current)	$27.1 \pm 2.5 \pm 1.6$	$94.5 \pm 8.0 \pm 5.3$	$276 \pm 20 \pm 14$
Yields in the measured kin range (previous)	$0.0214 \pm 0.0023 \pm 0.0024$	$0.0431 \pm 0.0034 \pm 0.0035$	$0.0561 \pm 0.0039 \pm 0.0047$
Yields in the full kinematic range (previous)	$0.0589 \pm 0.0063 \pm 0.0065$	$0.133 \pm 0.010 \pm 0.011$	$0.239 \pm 0.017 \pm 0.020$
$A$ cross section, MB, mb (previous)	$48.9 \pm 5.2 \pm 5.1$	$167 \pm 13 \pm 13$	$427 \pm 30 \pm 29$

	$T_0$ , MeV ( $C+C$ )	$T_0$ , MeV ( $C+Al$ )	$T_0$ , MeV ( $C+Cu$ )
Experiment (current)	$114 \pm 14 \pm 9$	$129 \pm 15 \pm 10$	$121 \pm 15 \pm 10$
DCM-QGSM (current)	115	122	121
UrQMD (current)	100	118	124
Experiment (previous)	$98 \pm 24 \pm 25$	$157 \pm 24 \pm 12$	$160 \pm 27 \pm 21$
DCM-QGSM (previous)	122	129	131
UrQMD (previous)	107	127	132

**Table.** Comparison between temperatures parameters for 4A GeV.

# $p_T$ spectra of $\Lambda$ : MC predictions in 4A GeV C+A (update)

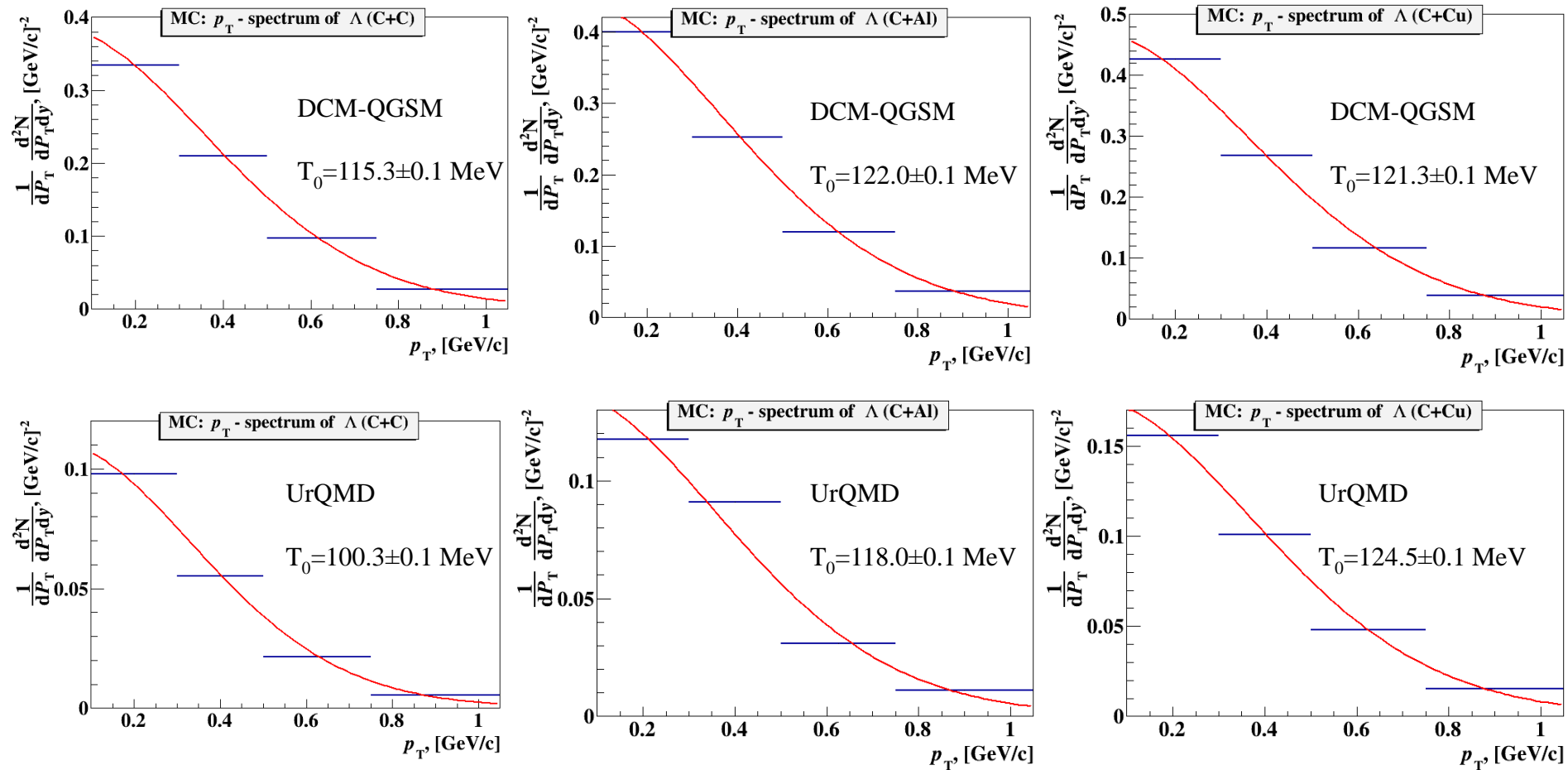


**Fig.** Fit of the DCM-QGSM and URQMD spectra. The inverse slope parameter  $T_0$  is shown, extracted from the fit.

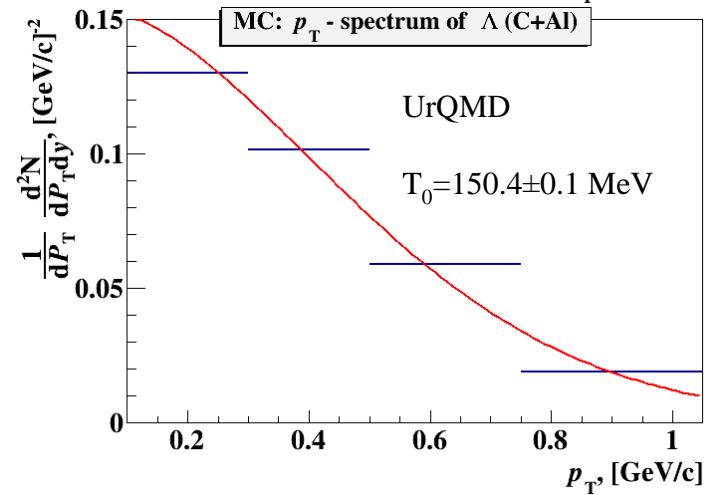
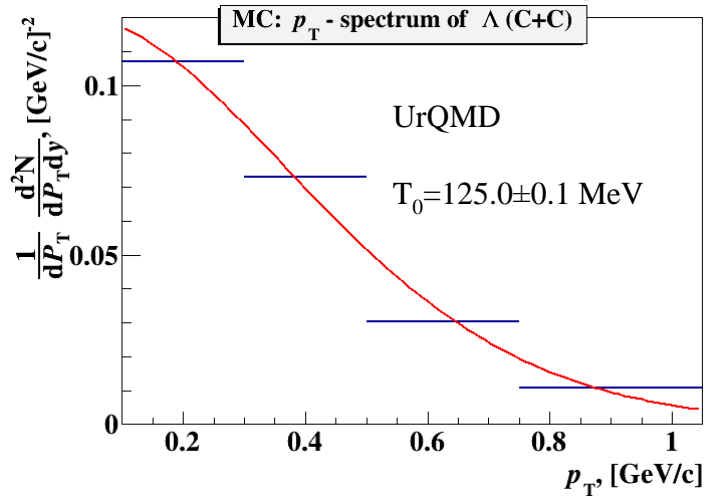
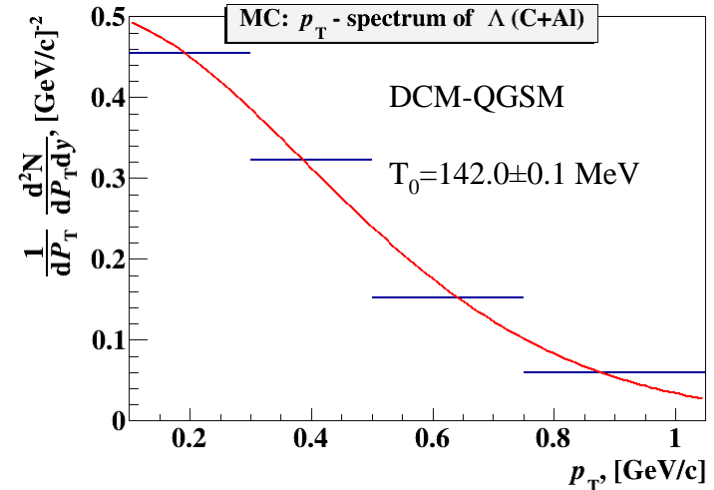
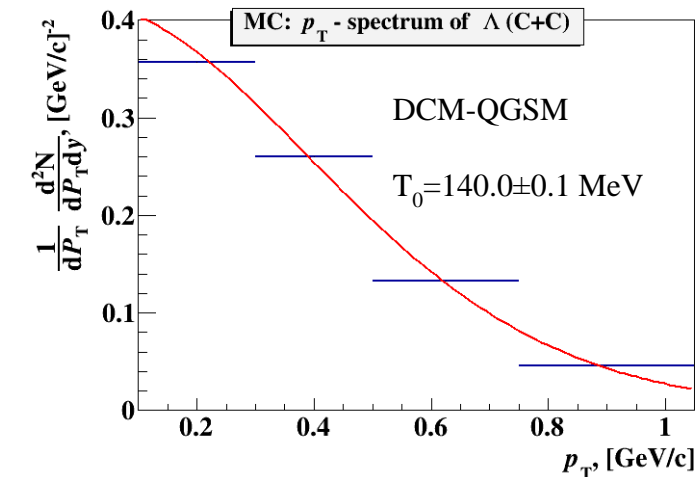


**Fig.** Fit of the DCM-QGSM and URQMD spectra. The inverse slope parameter  $T_0$  is shown, extracted from the fit.

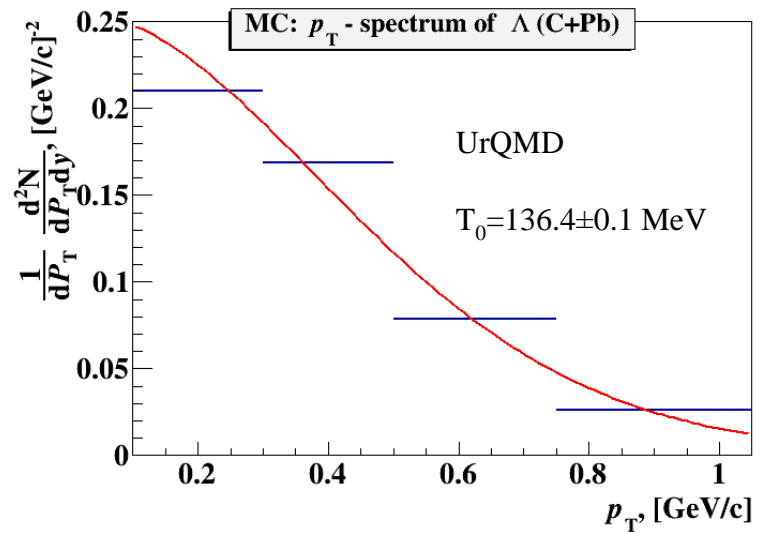
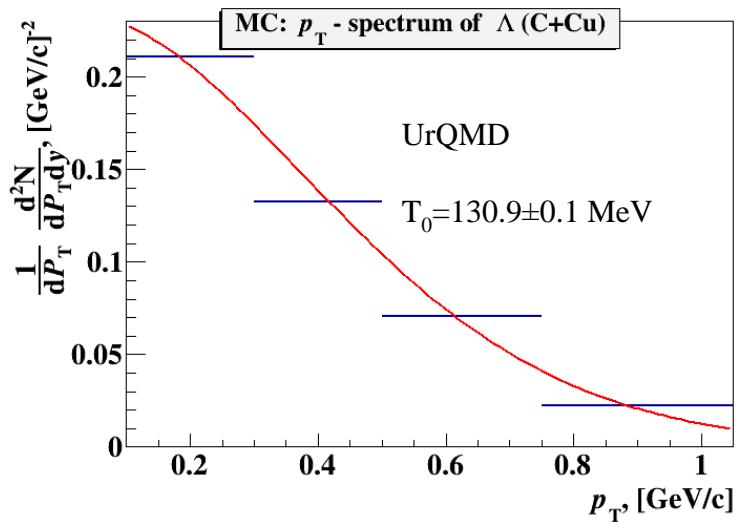
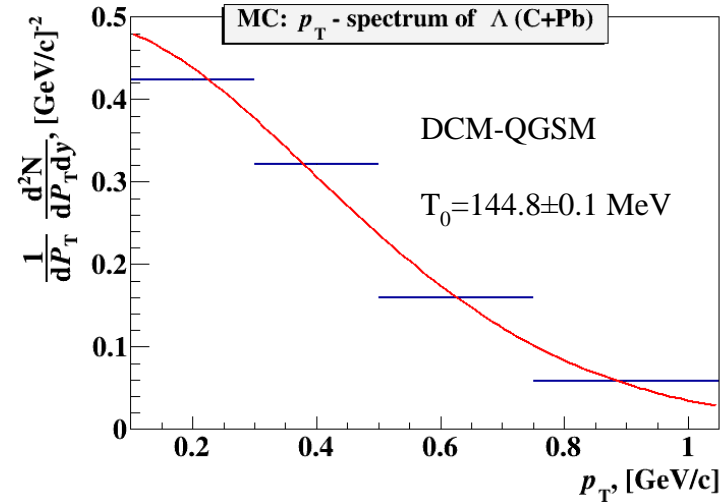
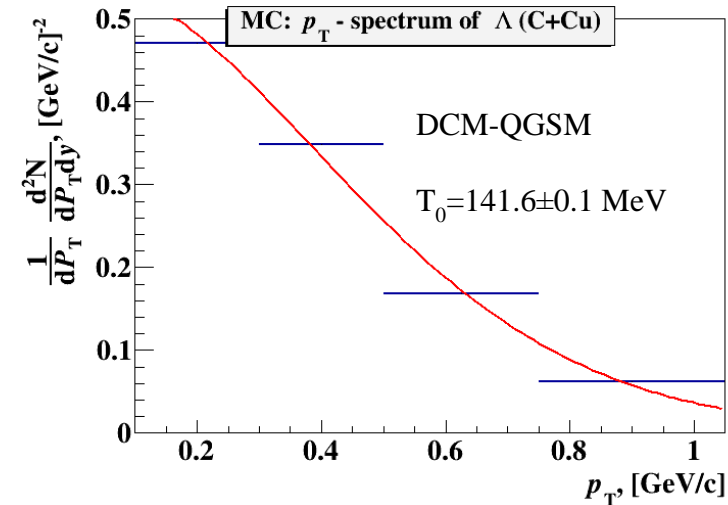


**Fig.** Fit of the DCM-QGSM and URQMD spectra. The inverse slope parameter  $T_0$  is shown, extracted from the fit.

# Triggers and impact parameters



**Table.** Trigger efficiency evaluated for events with reconstructed  $\Lambda$  hyperons in interactions of the carbon beam with  $C$ ,  $Al$ ,  $Cu$  targets. The systematic errors take into account the uncertainty due to the delta electron background. The last row shows the trigger efficiency averaged over the data samples with trigger conditions  $BD \geq 2$  and  $BD \geq 3$ .

Trigger / Target	$C$	$Al$	$Cu$	$Pb$
$\epsilon_{\text{trig}} (BD \geq 2)$	$0.906 \pm 0.010$ $0.870 \pm 0.020$	$0.955 \pm 0.010$	$0.904 \pm 0.01$	
$\epsilon_{\text{trig}} (BD \geq 3)$		$0.923 \pm 0.020$ $0.890 \pm 0.020$	$0.883 \pm 0.02$ $0.930 \pm 0.02$	$0.950 \pm 0.02$
$\epsilon_{\text{trig}}$ averaged		$0.940 \pm 0.015$	$0.893 \pm 0.015$	

# Yields of $\Lambda$ hyperons in 4A GeV C+A(previous)

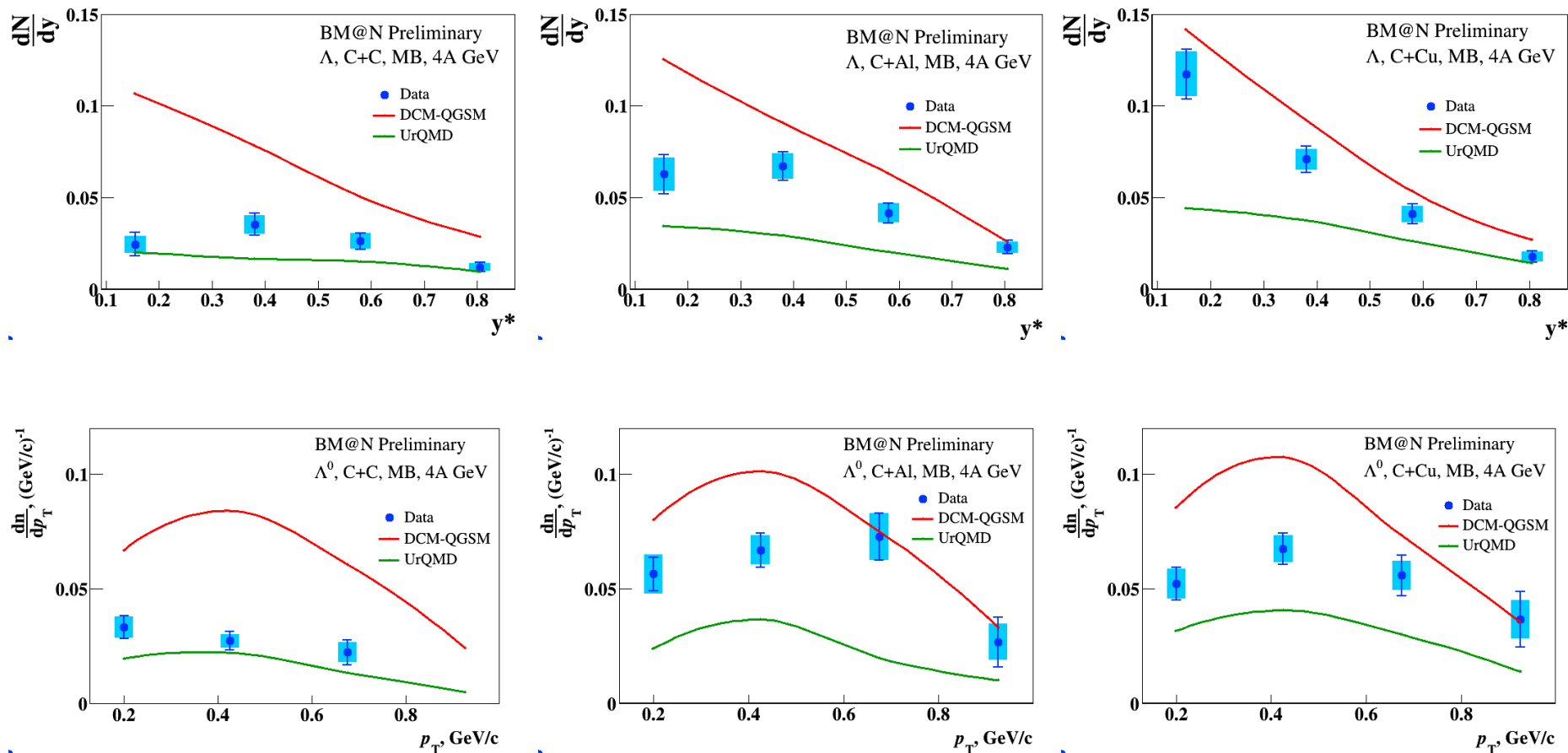


**Fig.** Reconstructed yields of  $\Lambda$  hyperons in minimum bias C+C, C+Al, C+Cu interactions vs rapidity  $y$  and transverse momentum  $p_T$ .

# $p_T$ spectra of $\Lambda$ and $T_0$ slope in 4A GeV C+A(previous)

**Table.** Temperature parameter extracted from the fit of the  $p_T$  spectra.

	$T_0$ , MeV (C+C)	$T_0$ , MeV (C+Al)	$T_0$ , MeV (C+Cu)
Experiment	$98 \pm 24 \pm 25$	$157 \pm 24 \pm 12$	$160 \pm 27 \pm 21$
$\chi^2$ /ndf	2.04/1	2.51/2	0.39/2
DCM-QGSM	122	129	131
UrQMD	107	127	132

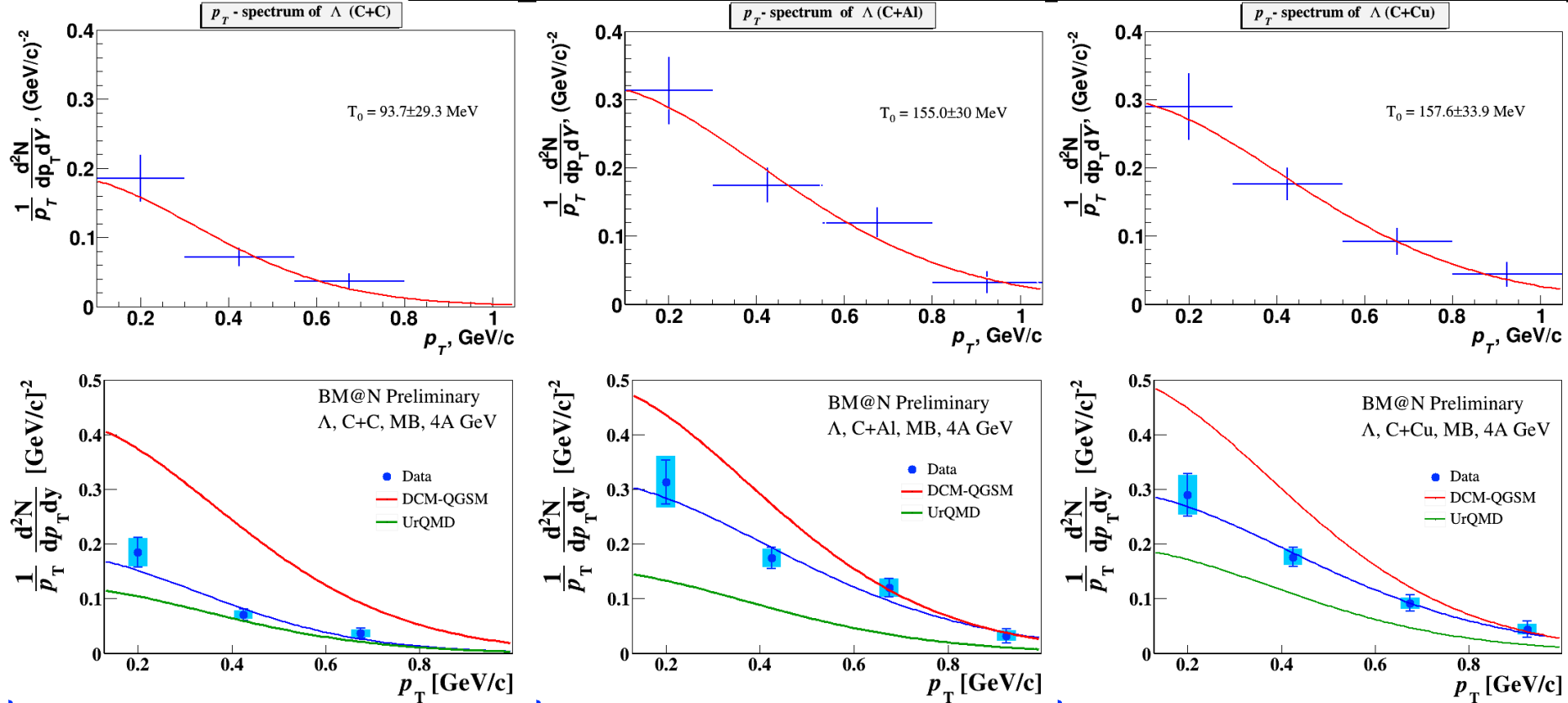


**Fig.** Thermal fit results with the inverse slope parameter  $T_0$ : data and predictions of models.

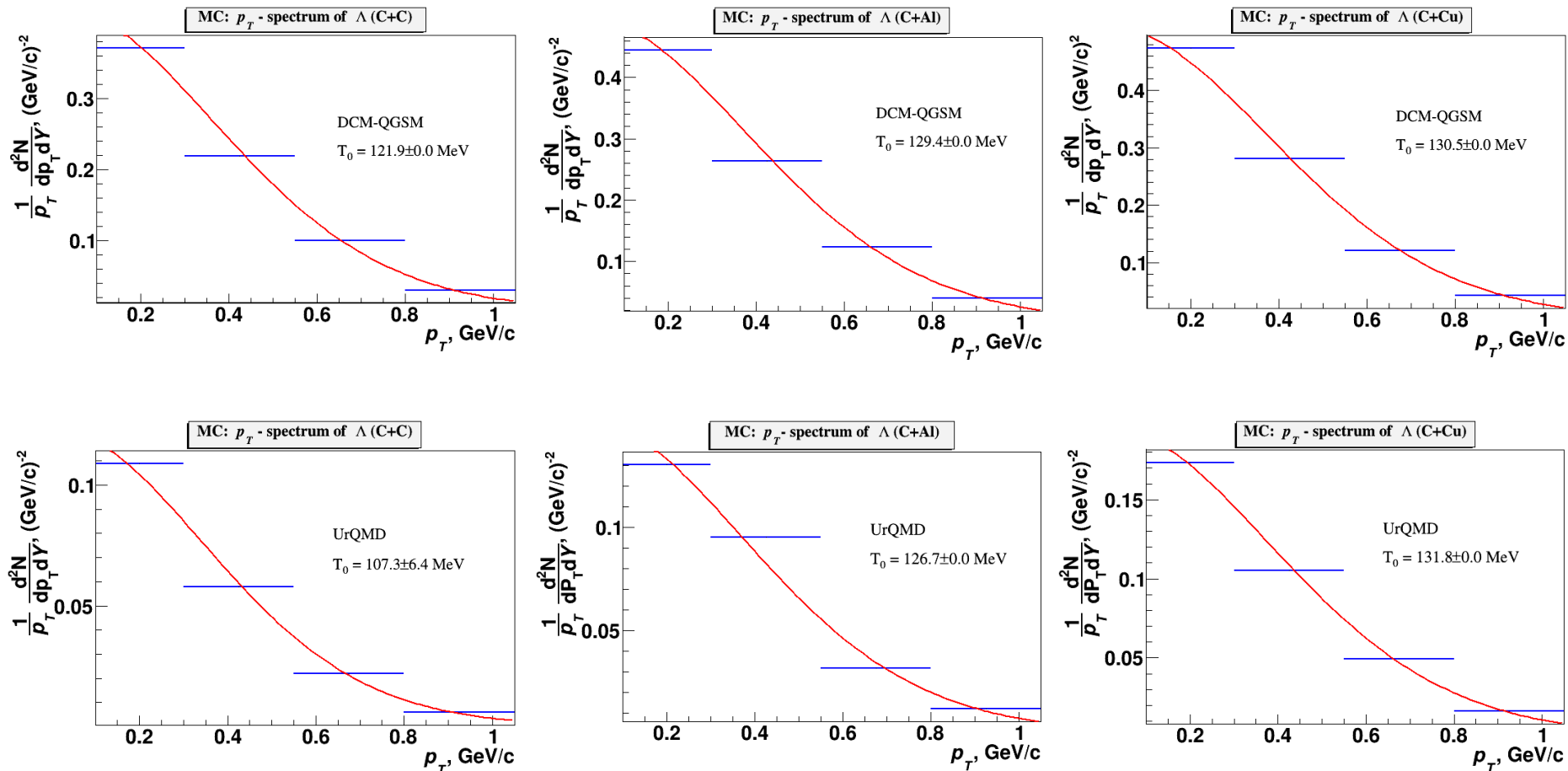


**Fig.** Fit of the DCM-QGSM and URQMD spectra. The inverse slope parameter  $T_0$  is shown, extracted from the fit.



**Table.** Extrapolation factors to the full kinematic range, yields and cross sections.

	<i>C</i>	<i>Al</i>	<i>Cu</i>
DCM-QGSM URQMD extrapolation factors	6574/2474 1827/639	10539/3413 3248/1056	15817/3545 5509/1360
Yields in the measured kin range $0.1 < p_T < 1.05$ GeV/c, $1.2 < y_{lab} < 2.1$	$0.0214 \pm 0.0023 \pm 0.0024$	$0.0431 \pm 0.0034 \pm 0.0035$	$0.0561 \pm 0.0039 \pm 0.0047$
Yields in the full kinematic range N part DCM-QGSM	$0.0589 \pm 0.0063 \pm 0.0065$ 9	$0.133 \pm 0.010 \pm 0.011$ 13.4	$0.239 \pm 0.017 \pm 0.020$ 23
<i>A</i> cross section in min. bias interactions, mb	$48.9 \pm 5.2 \pm 5.1$	$167 \pm 13 \pm 13$	$427 \pm 30 \pm 29$

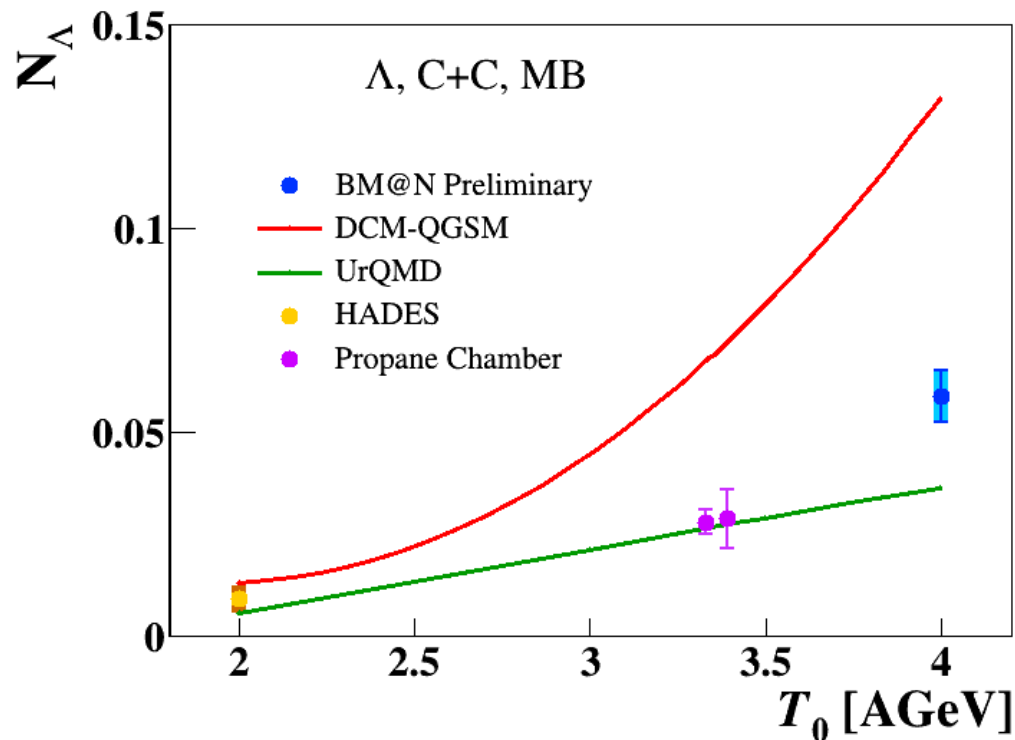


**Fig.** Energy dependence of  $\Lambda$  yields measured in different experiments. BM@N result is compared with data [S.Arakelian *et al.*, P1-83-354, JINR, Dubna; D.Armutlijsky *et al.*, P1-85-220, JINR, Dubna; Kalliopi Kanaki, PhD “Study of  $\Lambda$  hyperon production”]. The predictions of the DCM-QGSM and UrQMD models are shown.

# Signal of $\Lambda$ in $C+C$ , $C+Al$ , $C+Cu$ interactions

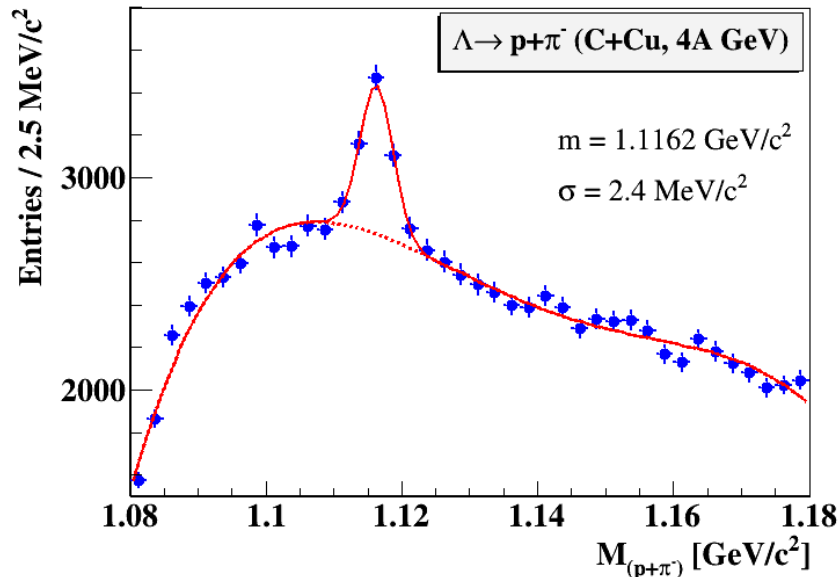
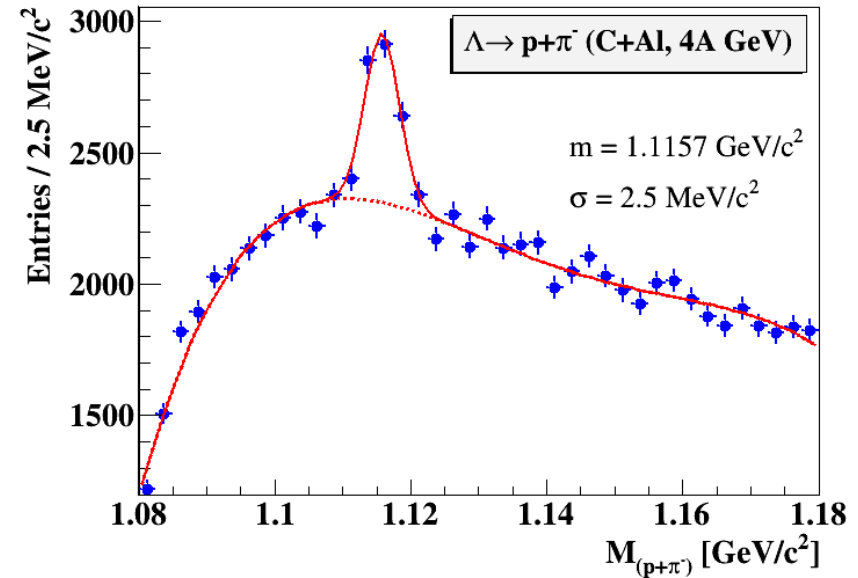
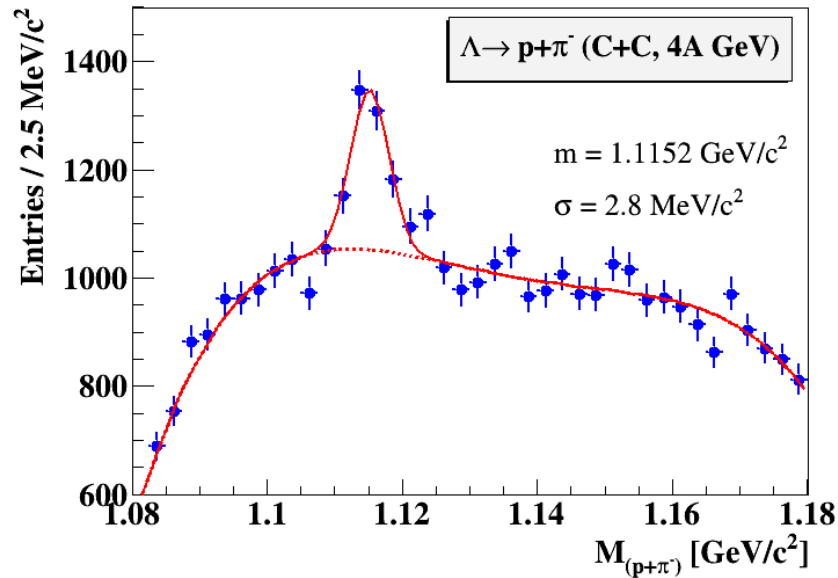


**Fig.**  $\Lambda \rightarrow p\pi^-$  signal reconstructed in interactions of the carbon beam with targets:  $C$ ,  $Al$ ,  $Cu$ .

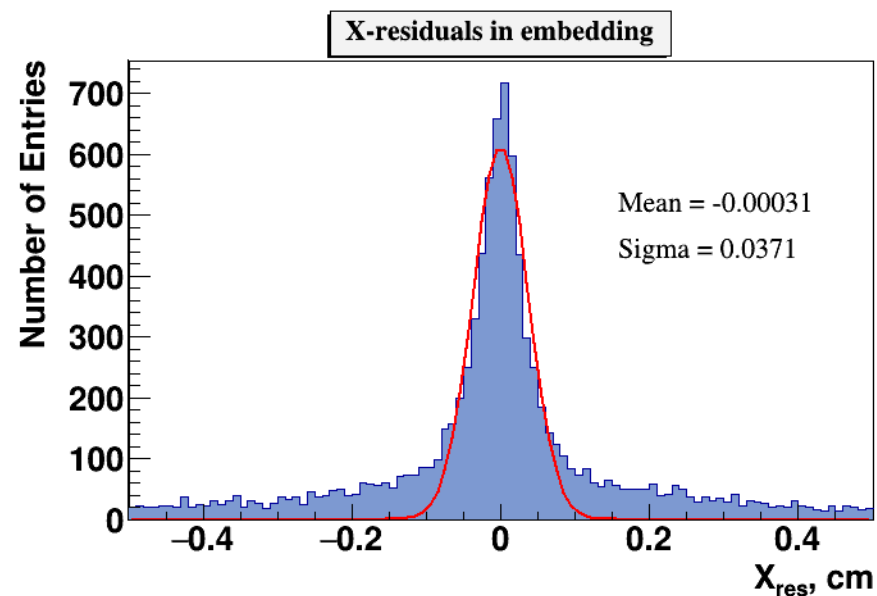
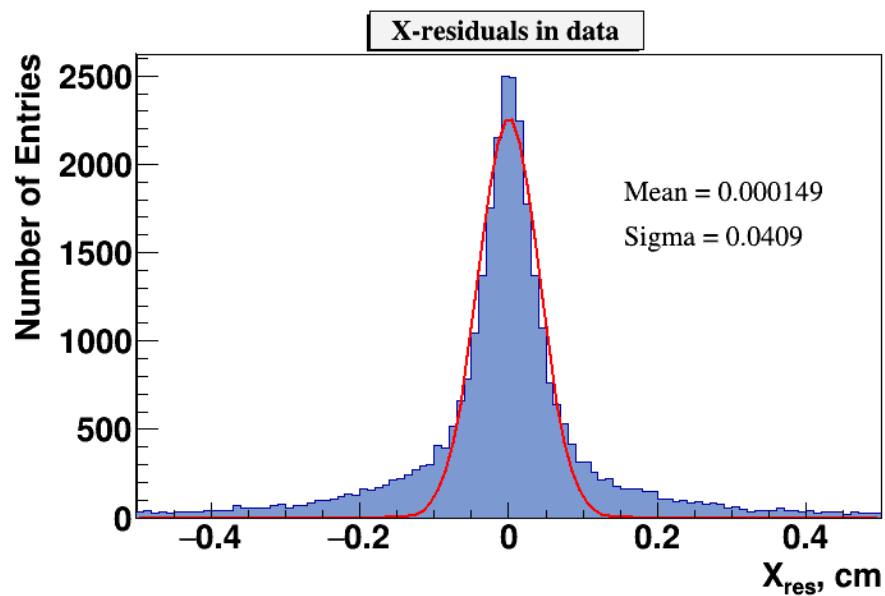


**Fig. 12.** Residual distributions of GEM hits with respect to reconstructed tracks: left) experimental data, right) reconstructed tracks of embedded  $\Lambda$  decay products.

# The invariant mass spectrum

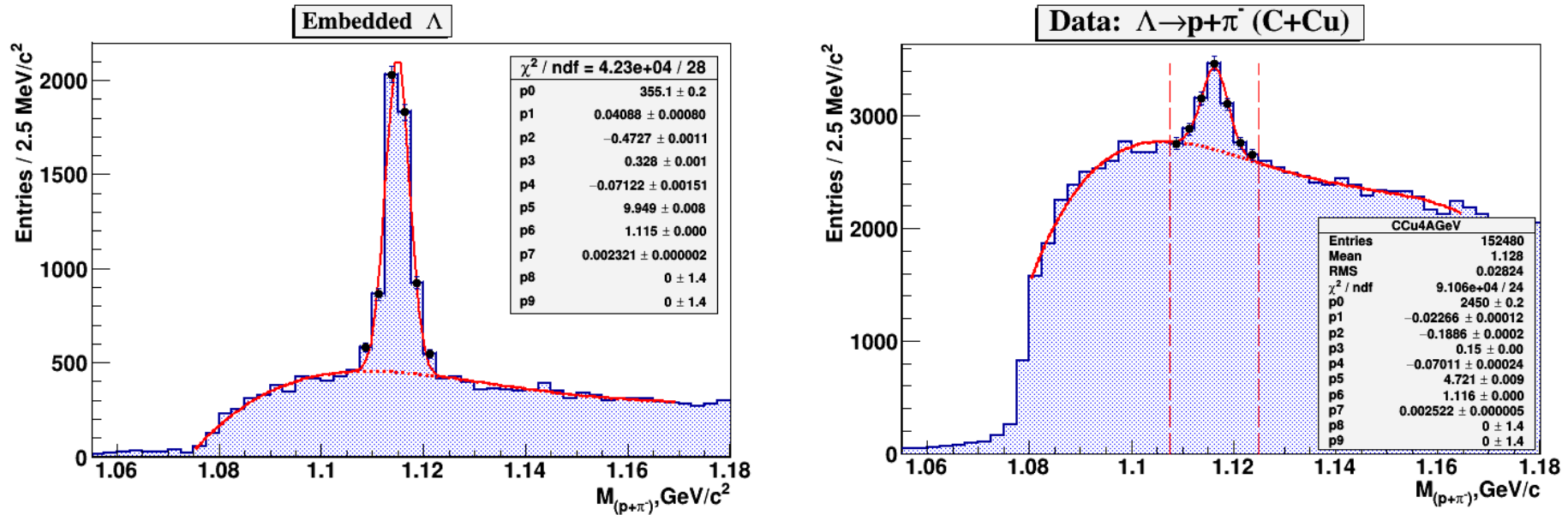


**Fig. 13.** The invariant mass spectrum of  $(p, \pi)$  pairs reconstructed in the experimental events of  $C+Cu$  interactions with embedded  $\Lambda$  hyperon decay products (left); The invariant mass spectrum of  $(p, \pi)$  pairs reconstructed in  $C+Cu$  interactions (right).

# The $\Lambda$ yields and production cross section



Interacting nucleus / reference	Beam momentum, kinetic energy ( $T_0$ )	$\Lambda$ cross section, mb	$\Lambda$ yield, $\cdot 10^{-2}$
$He_4+Li_6$	4.5 GeV/c (3.66A GeV)	$5.9 \pm 1.5$	$1.85 \pm 0.5$
$C+C$	4.2 GeV/c (3.36A GeV)	$24 \pm 4$	
$C+C$ , propane chamber	4.2 GeV/c (3.36A GeV)		$2.8 \pm 0.3$
$p+p$	4.95 GeV/c (4.1 GeV)		$2.3 \pm 0.4$
$C+C$ , HADES	2A GeV	$8.7 \pm 1.1 \pm^{3.2}_{1.6}$	$0.92 \pm 0.12 \pm^{0.34}_{0.17}$
$Ar+KCl$ , HADES	1.76A GeV		$3.93 \pm 0.14 \pm 0.15$
$Ar+KCl$ , FOPI	1.93A GeV		$3.9 \pm 0.14 \pm 0.08$
$Ni+Ni$ , FOPI, central 390 mb from 3.1 $b$	1.93A GeV		$0.137 \pm 0.005 \pm^{0.009}_{0.025}$
$Ni+Cu$ , EOS, full $b < 8.9$ fm / central $b < 2.4$ fm	2A GeV	$112 \pm 24 / 20 \pm 3$	
$Ar+KCl$ , central $b < 2.4$ fm	1.8A GeV	$7.6 \pm 2.2$	